CRACK INITIATION AND GROWTH BEHAVIOR AT CORROSION PIT IN 2024-T3 ALUMINUM ALLOY

THESIS

Al-Qahtani, Ibrahim.

First Lieutenant, Royal Saudi Air Force, RSAF

AFIT-ENY-T-14-S-05

DEPARTMENT OF THE AIR FORCE
AIR UNIVERSITY

AIR FORCE INSTITUTE OF TECHNOLOGY

Wright-Patterson Air Force Base, Ohio

DISTRIBUTION STATEMENT A

APPROVED FOR PUBLIC RELEASE; DISTRIBUTION IS UNLIMITED

The views expressed in this thesis are those of the author and do not reflect the official policy or position of United States Air Force, Department of Defense, the United States Government, the corresponding agencies of the Saudi Arabian Air Force, the Department of Defense, or the Saudi Arabian Government or any other defense organization.

AFIT-ENY-T-14-S-05

CRACK INITIATION AND GROWTH BEHAVIOR AT CORROSION PIT IN 2024-T3 ALUMINUM ALLOY

THESIS

Presented to the Faculty

Department of Aeronautics and Astronautics

Graduate School of Engineering and Management

Air Force Institute of Technology

Air University

Air Education and Training Command

In Partial Fulfillment of the Requirements for the

Degree of Master of Science in Materials Science

Al-Qahtani, Ibrahim.
First Lieutenant, Royal Saudi Air Force, RSAF

September 2014

DISTRIBUTION STATEMENT A

APPROVED FOR PUBLIC RELEASE; DISTRIBUTION UNLIMITED

AFIT-ENY-T-14-S-05

CRACK INITIATION AND GROWTH BEHAVIOR AT CORROSION PIT IN 2024-T3 ALUMINUM ALLOY

Al-Qahtani, Ibrahim.
First Lieutenant, Royal Saudi Air Force, RSAF

Approved:

//signed//	23 June 2014
Shankar Mall, PhD (Chairman)	Date
//signed//	17 June 2014
Lt Col Timothy C. Radsick, PhD (Member)	Date
//signed//	23 June 2014
Vinod K. Jain, PhD (Member)	Date

Abstract

In this research, fatigue crack formation from two types of corrosion pits at a circular hole was investigated under uniaxial fatigue. Through pits and corner pits were created on the edge of a circular hole in test specimens using an electrochemical process. Specimens of 2024-T3 aluminum alloy were subjected to cyclic uniaxial loads with stress ratio of R = 0.5 in both air and saltwater environments. A fracture mechanics approach was used to investigate the crack initiation and crack growth from corrosion pits. Specimens with a through pit at the edge of a circular hole had a closed form solution to predict stress intensity factor range, ΔK, which was in agreement with finite element analysis. In addition, specimens with a corner pit do not have a closed form solution and finite element modeling was used to determine stress intensity range. Optical and electron microscopy provided an accurate method to measure the size of corrosion pits. Exposure to saltwater reduced the number of cycles for crack initiation in both types of corrosion pits. This reduction is up to 90% for through pits and up to 75% for corner pits. The required number of cycles for crack initiation for corner pit specimens is less than for through pit specimens. Here, the number of cycles decreases up to 94% in air and up to 88% in saltwater environment. There was a good agreement between crack growth rates in machined notch specimens and the specimen with through pit.

Acknowledgments

First, I would like to thank my advisor, Dr. Shankar Mall, for giving me the opportunity to work on this project. I appreciate his technical insights, guidance, and dedication to his students.

Also, I would like to thank for Dr.Volodymyr Sabelkin for taking the time to show me how to properly prepare specimens and execute fatigue experiments, Dr. Victor Perel for his help in developing the finite element models, and Dr. Heath Misak for showing me how to capture the beautiful SEM images of the fatigue specimens.

Additionally, I would like to thank my parents and my eldest brother, for inspiring me to always do my best. They have always provided the best opportunities for me, and I appreciate their love and support during this undertaking.

My special thanks go out to Captain Zafer Dolu for his support and friendship during all my thesis work.

I would also like to acknowledge the support of this work from the Technical Corrosion Collaboration (TCC), Office of Secretary of Defense (OSD), Washington D.C

Al-Qahtani, Ibrahim.

Table of Contents

Page

List of Figures

Page

List of Tables

Page

List of Symbols

Symbol	Definition
a	crack length (mm)
b	width of specimen (mm)
C	constant for Paris law (unit less)
E	electric potential (Volts)
F	applied load (Newtons)
F	Faraday's Constant (C/mol)
I	current (Amps)
K	stress intensity factor (MPa*m^0.5)
R	stress ratio for cyclic loading (unit less)
Q	charge (Coloumbs)
P	applied load (Newtons)
n	number of moles (Moles)
w	width of specimen (mm)
t	thickness of specimen (mm)
σ	stress (MPa)
da/dN	rate of crack growth per cycle (mm/cycle)
Δ	change in a variable (unit less)
min	minimum load values
max	maximum load
I	mode one (opening)
cell	electrochemical cell

anode	anodic reaction
cathode	cathodic reaction
t	designates stress concentration factor

Superscripts

m	constant for Paris law (unitless)
−	anode
n+	cathode

CRACK INITIATION AND GROWTH BEHAVIOR AT CORROSION PIT IN 2024-T3 ALUMINUM ALLOY

1. Introduction

1.1 Corrosion and Fatigue Effects

The most essential aspects of human life in the modern era, including infrastructure and industrial growth, are dependent on technology. The latter is growing at a faster pace than anticipated. Corrosion is a great concern in all industries since corrosion affects the longevity of products, hence reducing the design life, cost and efficiency. Corrosion also leads to loss, efficiency and contamination of products. The United States Air Force (USAF) has a great deal of concerns with respect to fatigue and cracking that costs the United States (US) billions of dollars annually in order to overcome the effects of fatigue and corrosion cracking for safety, economy and conservation of USAF property. Metal corrosion is caused by exposure to chemicals and oxides, most commonly by exposure to the environment [30].

Corrosion is defined as the deterioration of a metallic material caused by a reaction between the metal and its environment or surroundings in the presence of an electrolyte, cathode, anode and an electric circuit. Corrosion can be mitigated by the use of several methods, including coatings, chemical inhibitors, non-corrosive or stainless steel materials selection, protection by cathode, etc. Proper understanding of corrosion is crucial for the development of corrosion prevention methods. The dissolution of metal occurs at anode

and the process starts in the presence of cathode, therefore the corrosion reaction can be mathematically described as follows [13, 30]:

$$\text{General anodic reaction:} \quad M(s) \rightarrow M^{n+} + ne^{-} \tag{1.1}$$

$$\text{General cathodic reaction:} \quad M^{n+} + ne^{-} \rightarrow M(s) \tag{1.2}$$

These equations show that electrons are transferred between the metal and its environment to create ions and excess electrons. These reactions must occur in an electrolytic solution to allow for the transfer of electrons. For this process there must be an anodic surface which will donate the electrons and a cathodic surface which accepts these electrons [13].

One of the most important metals that is highly resistant to corrosion is aluminum. It is widely used because it is highly efficient and economical. The oxide film that develops on the aluminum alloys acts as a barrier in protecting the alloy from different environmental factors. Therefore, aluminum alloy can be used even in aggressive environment as it can re-form easily from any attack or loading that causes deformation. In general, the corrosion reaction is spontaneous and the reaction occurs in acid solutions because of the proton reduction and oxidation. Aluminum alloy is strongly affected by corrosion only in highly concentrated acidic solutions. In aqueous solutions that are neutral, the oxide film helps in protecting the alloy from passive reactions [9].

The USAF is undertaking a great part of research to enhance and control the cause of fatigue and corrosion cracking as the designed life period of the USAF fleet has to serve its purpose and also reduce the cost of operations and maintenance. Aircraft components

under repetitive cyclic loading in corrosion environments often suffer from fatigue failure. Fatigue cracking over time develops into physical failure, affecting the metal body of the aircraft and thus affecting the service life of the aircraft. Structural design in the early development of aircraft was on strength, but now designers also deal with safety, corrosion fatigue and maintenance etc. Fatigue is of high concern as the attack of fatigue is seldom seen or noticed until failure occurs. Corrosion fatigue implies that a metal/body is exposed to a harsh environment in order to cause a corrosive reaction. Environment plays a vital role as a catalyst since it contains water in form of vapors and oxygen, which are sufficient for the aircraft to be affected by corrosion fatigue, as the aircrafts are meant to spend most of their life in such environment. There are many such other sources that are found in environment that affect the pitting and fatigue crack growth [19, 31]. Several research programs have been approved by the US government regarding fatigue cracking. The aircrafts' sustainability required understanding the behavior and growth of corrosion fatigue, crack initiation, crack growth; which leads to the need of systematic approaches and the understanding of factors that affect operations and service life. Figure 1.1 shows the annual (approximated) corrosion costs for different industry sectors.

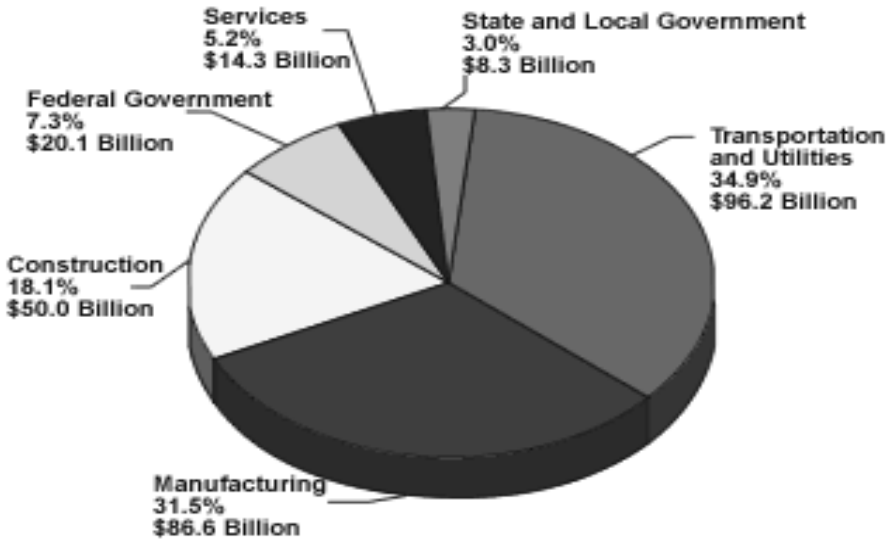

Figure 1.1: Annual approximate corrosion costs [17].

1.2 Corrosion Types

There are many ways that corrosion causes failure. In general, corrosion is characterized into two forms: localized and generalized. Corrosion occurs on the surface of the metal causing corrosion pits which help in the formation and initiation of cracks. Corrosion pits form on the surface and act as a starting point for the crack to grow and corrode the entire body. Crack development on the surface is generally caused due to oxidative attack of oxides on the metal, and is observed everywhere in the environment [10]. The atmosphere helps in the development of a corrosion pit and it can be identified over the period of time; therefore preventive measures can be taken. Hydrogen embrittlement from the atmosphere itself is enough to cause cracks; hydrogen is a small element and as a result, it attacks on the metal body of the aircraft and it is difficult to prevent such contamination. Corrosion attacks in a non uniform fashion, leading to the

development of pitting, corrosion at cracks, internal corrosion and galvanized corrosion; which results in dangerous metal degradation such as on the aircraft's body parts [4, 13]. Corrosion fatigue implies that a metal must be exposed to a harsh corrosive environment in order to cause corrosion pit which develops into crack, as shown in Figure 1.2.

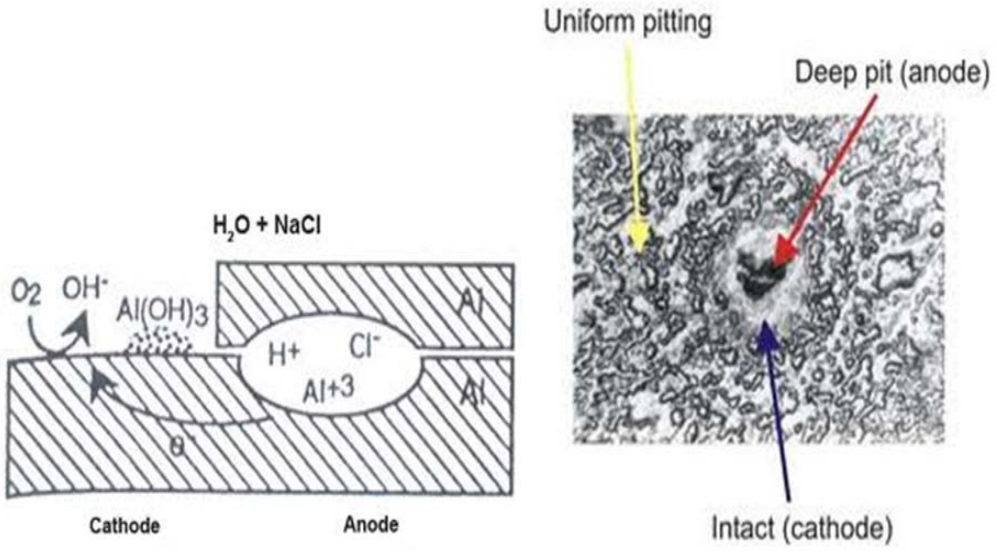

Figure 1.2: Types of corrosion and pit formation [33].

Corrosion fatigue is also an important parameter for crack formation that leads to failure of the metal due to repeated and cyclic loading along with an intense corrosive environment. This repeated and cyclic loading process is called fatigue failure. In general, corrosion pits may not be noticed until complete failure of aircraft [6, 33]. This leads to an important aspect of this research: the effects of crack initiation due to corrosion pit and fatigue.

1.3 Background

The development of a crack or the process of crack initiation starts at corrosion pits and propagate deep into the metals and over time leads to the failure of a part or of the entire body [5, 38]. An extensive amount of research has been conducted on the metals that are typically used for structural purposes. In the aircraft industry, there are few materials that used in aircraft structure, and aluminum alloy is one of those metals. Aluminum alloy has great strength and great endurance when subjected to repetitive loading. The research by McEvily explains the crack growth caused by fatigue that developed from the corrosion pits [18]. Most of his work deals with corrosion crack propagation in aluminum alloy. It is important to know about fatigue and corrosion individually, but it is much more useful to explore how both processes work together during crack growth. Studies from numerous research laboratories used aircraft type loading (tension-tension loading) to determine that, not surprisingly, fatigue life decreases in the presence of a corrosive environment [6, 9, 31, 38]. While this information is very useful, these studies focused primarily on the crack growth after the initiation of the man-made crack. In other words, they focused on the crack growth after the crack has formed. Some research in this area has been conducted, but the extent of this research is limited when compared to the previously mentioned research topics.

The development of cracks from corrosion pits needs to be understood because it deals with both fatigue crack initiation and growth which requires concepts of fracture mechanics. Corrosion crack initiation or growth can develop when exposed to continuous or intermittent humid environment during the service. Once corrosion pits are formed, cracks will initiate and propagate and the failure in many engineering structures are observed due

to these cracks that are formed and developed by corrosion pits [19, 24]. Small corrosion pit formations that cause loss of metal can develop into a major issue that may lead to failure of the aircraft. These corrosion pits that cause crack initiation due to anodic and cathodic reactions may not be seen immediately [10, 29]. Corrosion pits are often small in appearance near the surface and may be large when crack initiation propagates deeper into the metal. In many studies the concept of fracture mechanics has been used. For example, Lee and Dorman [20] concentrated on the crack growth rate of corner pit on a hole and cycles that were required to cause them, in their study. They used the fracture mechanics to estimate initial stress intensity range. The rest of the crack growth is specified only as a function of the number of cycles. As a result, there is a need to investigate not only the transition from corrosion pit to fatigue crack growth, but also to study this transition using fracture mechanics principles.

1.4 Problem Statement

Understanding of the transition from a corrosion pit to a fatigue crack is a very important issue. The focus of the current research is in this area. There have been many researches already completed for crack growth and pit formation individually [4, 5, 8, 11, 36], but further research is required to examine the interactions between the two studies using the fracture mechanics principles. Furthermore, more research is necessary for the crack growth in specimens that have pits that exist at holes. Since there has been no study on both crack initiation and growth behaviors of 2024-T3 at corrosion pit, in this study these behaviors will be investigated. For the experiments, 50.8 mm wide and 3.2 mm thick aluminum specimens with 6 mm diameter circular holes at the center were machined. Two

types of corrosion pits were electrochemically created at the hole edge and subjected to uni-axial fatigue with stress ratio of 0.5 in both ambient air and saltwater (3.5% NaCl) environments. A high magnification camera was used to observe and measure the crack initiation and growth per cycle. Additionally, the scanning electron microscope was used to examine the fracture surfaces. Finite element analyses were conducted to calculate the stress intensity factor range. These ranges were then correlated with the measured crack initiation life and crack growth rates. This research provided understanding of transition from corrosion pit to long crack in both air and saltwater environments. Current research emphasizes fatigue crack initiation and growth behaviors from a corrosion pit on the 2024-T3 aluminum alloy. This study will provide a great deal of useful information for fatigue crack initiation and growth from a corrosion pit and will make useful data for uniaxial loading to better predict the lifetimes of an aging fleet of aircraft, and finally will help to fill the void that exists from previous studies [4, 5, 8, 11, 13, 25, 36].

2. Background

2.1 Corrosion Theories

Aluminum alloy containing noticeable amounts of soluble alloying elements such as zinc, magnesium are susceptible to stress corrosion cracking (SCC), an analysis of failure shows the way these serviceability failures occurred and the kind of reaction led to the initiation and propagation of stress corrosion cracks that caused failure. Alloys such as 7079-T6, 7075-T6 and 2024-T3 have contributed more than 90% of failures that have occurred due to service failure of all high strength aluminum [5]. Corrosion is a problem as it is energetically favorable for an alloy to return to its oxidized state from cultivated state as energy is required to create metals for both the mentioned cases. Systems as explained in thermodynamics are attracted towards states of higher entropies of disorder and energy of lower levels, thus resulting that any metal will linearly reach a corroded state and the best that could be done is to protect and try to reduce the possibility of occurrence of corrosion and if corroded replacing the affected metal parts would prevent any disastrous events. Electrochemistry and thermodynamics explain the theory of corrosion as corrosion is a process that evolves naturally.

The electrochemical theory of stress corrosion was developed in 1940 to explain stress corrosion. The theory defines the electrochemical reaction occurs when a transfer of electrons takes place, resulting in oxidation and reduction. Oxidation is a process in which a metal tends to lose electrons during the reaction and reduction is a process in which a metal tends to gain electrons. This phenomenon of losing or gaining of electrons is known as electrochemical process, to explain in a more approachable way, basically a cathode, anode

and an electric circuit connecting them is required to cause corrosion. Dissolution of metal occurs on the node where the corrosion enters the electrolyte and propagates through cathode.

Electrolytic solution is required for this reaction to take place so that transfer of electrons is possible, for this process electron that are lost at anode flow through the metallic circuit towards the cathode and develop a cathode reaction. The same metal can consist of these anode and cathode regions and the presence of an electrolytic solution is required to complete this process as shown in Figure 2.1. A great deal of corrosion process takes places for electrochemical reactions. These regions of anode and cathode can also be adjacent to each other in a metal [5, 13].

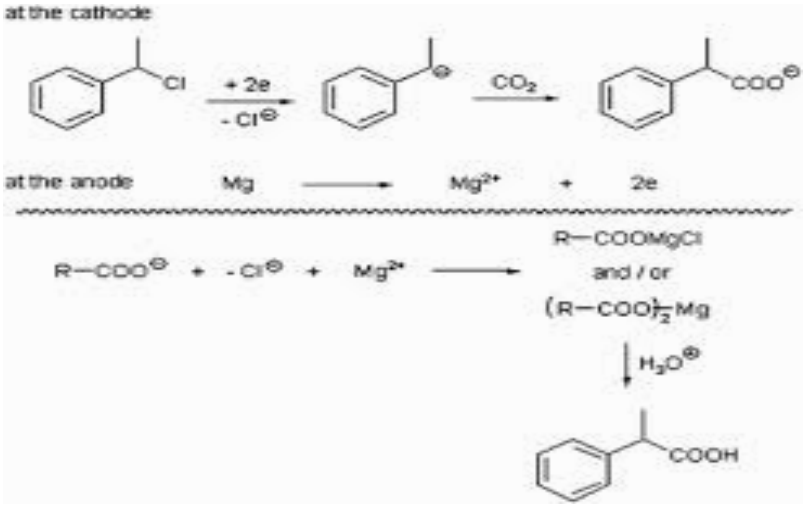

Figure 2.1: Reaction mechanism of electrochemical process [5].

The anodic and catholic regions may shift when the process of electrochemical reaction takes place, which explains that corrosion can occur in dissimilar metals which are

in proximity to each other. This is known as localized corrosion or galvanic corrosion. In other words, this type of corrosion is also called as metal to metal corrosion. This type of corrosion attacks the junction or connecting points where the metals are connected and this type of corrosion attack is caused due to metals of different composition are easily vulnerable to attacks. Presence of galvanic series, electrical contact or presence of an electrolyte causes galvanic corrosion attacks [9]. In this type of corrosion the electron transfer occurs when current is generated during reaction, where the loss of mass and rate of corrosion can be determined by using Faraday's law.

In Faraday's law a systematic relationship between the dissolution metal rate at any potential of a metal and the anodic partial density of current for metal dissolution is linear [3]. The moles of the metal that is corroded and the total amount of charge that is carried by the moles of that metal can be related by Faraday's law,

$$Q = F\Delta Nn \tag{2.1}$$

Where, 'F' is Faraday's constant, 'ΔN' is change in number of moles of the material, and 'n' is the number of electron per moles of the material. The rate or current is expressed by equation 2.3, in which 'I' is total current in amperes and 't' is the time/duration of the reaction expressed in seconds [12].

$$Q = \int_0^t Idt \tag{2.2}$$

To understand corrosion phenomenon the study of electrochemical thermodynamics and electrochemical kinematics has to be understood. The rate of corrosion depends on the

kinetics of an electrode and it is defined in general, if all parameters of electrochemical anodic and cathode partial reactions are known [12].

2.2 Pitting Corrosion

Pitting corrosion is a form of localized corrosion that produces attacks in the form of pits, crevices or spots. When there is loss of volume in a metal such that cavity or crack is formed on the surface that leads to formation of pits. When left unnoticed pits can propagate into the metal causing holes and thus destroying the metal. This type of corrosion is one of the affective and dangerous type of corrosion due to uncertainty of recognizing and forecasting of pits. Tiny pits can cause severe problems as the formation of it in a crucial place of the metal structure can lead to calamity and even cause loss of life. This is true and it is important to identify when pits are of shapes as explained in Figure 2.2.

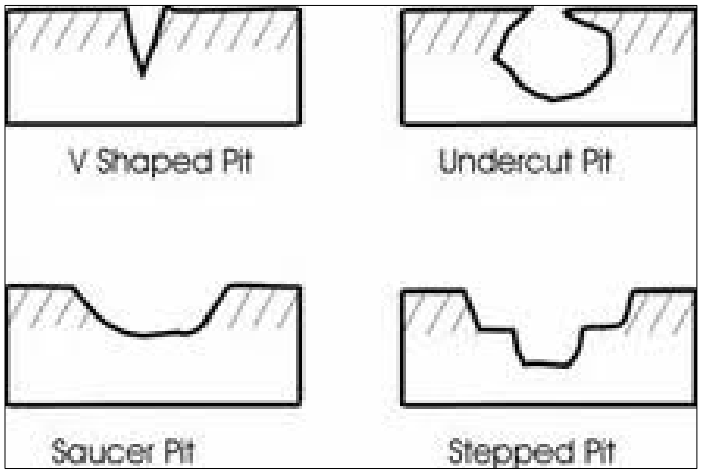

Figure 2.2: Different shapes of pits [34].

The formation of pits is observed where there is loss of a protective layer which is lost due scraping, removing or due to environmental conditions. This type of losing the

protective layer possesses a problem as certain area of any size when left unprotected influences in causing corrosion and as a result the rate of formation of corrosion pits tend to grow at an unexpected rate. Pitting corrosion may occur in alloys and metals in neutral or acid solutions containing chlorides and this type of corrosion occurs in place where the layer protected by passive nature might be deteriorated or damaged. Few types of attack can penetrate into great depth with a short period of time. Under conditions in the presence of chlorides and exaggerated temperatures pits may form on the surface of the metals and the propagation of these pits are dependent on the environment and type of corrosion attack and can lead to perforation. For metals that are passive in nature a uniform form of pitting corrosion is not usually formed or it is possible in the presence of more exaggerated environments [33]. These pits in time can cause an increase in parts of the metal that are corroded and lead to catastrophic failure.

The cracks known as fatigue cracks grow from these pits which act as nucleation sites. For many materials of the structure such as Al, steel the growth of fatigue cracks from corrosion pit stands legitimate and in positive conditions, even titanium can be affected due to this type of attack. It is observed that some values for the size of pits that are critical or rather threshold values below which the nucleation of fatigue crack is not possible [6]. Under certain conditions that prevail on surrounding defects the pit may develop into a crack though the size of pit is below the threshold value [31]. In pitting corrosion, the corrosion attacks start at the surface of the passive layer and develop into a crevice or crack corrosion that is more of a geometrical problem which may be of granular or inter-granular attacks. Presence of aggressive anions and the higher rate of equilibrium potential of the material called pitting potential cause passive materials naive enough to come under pitting

corrosion attacks. Metallography helps to identify the configuration of the pitting corrosion through which pit shape, pit depth, pit size and the area of the pit can be explained [13, 34].

Pits can also form in regions where the surfaces of anode and cathode are adjacent to each other. In general the identification of pits can be done by detecting the regions of cathode which are not corroded. This kind of identification may be difficult as the protective layer can cover the regions of cathode leading to change in place or change in geometry. The formation of ions of hydrogen on the surface of the material is formed in this type of a localized reaction of cathode. Thus formed hydrogen, which is unwanted, can travel to pit and cause embrittlement developing lattice structures [24]. This process, called hydrogen embrittlement causes the metal to weaken and is sufficient to cause initiation of cracks under cyclic loading [13, 30].

2.3 Fatigue Corrosion

Corrosion fatigue is important and the mode of failure caused by it is complex in nature for the metals which are used for high performance in tedious and detrimental environments. The application of cyclic varying loads on any structure and in the presence of active chemical environments that need for longevity of the design period of any structure is important. The prediction of the long term life component performance under these cyclic loads and environmental factors is high importance. Corrosion fatigue is defined as the damage of a metal or sometimes the whole body due to accumulated and repetitive loading cycle in attendance of chemically active environment. In the past, corrosion fatigue has affected airspace systems, power systems, nuclear systems, turbines, pipelines, marine constructions and many more industries. The importance of experimental

methods, design and loading, formation of cracks and measurement and other related aspects are to be exemplified in order to overcome corrosion fatigue. Moreover, electrochemical environments and mechanical experiments and result analysis regarding fatigue can be helpful in understanding the concept of corrosion fatigue. Simultaneous loading accompanied by tensile stresses and aggressive environment leads to initiation of corrosion cracking which is caused due to fatigue failure mechanisms. The process of fatigue is assumed to cause rupture or damage to the protective passive film, which causes an acceleration of corrosion and helps in forming pits or crevices. Corrosion fatigue failure may cause even at lower rates of loading and at a much faster pace of time [19]. The fracture caused by fatigue is mostly brittle and the crevices formed as trans-granular. When stresses are applied at high frequency fine cracks are formed. Importance in understanding the mechanisms behind corrosion fatigue is necessary in order to interpret the lab results. Corrosion fatigue is similar to stress corrosion cracking in many ways, such as rupture, re-passivation and other aspects [34]. Size and shape play an important role in formation of crack growth and once the size passes the point it has a comparatively less effect on crack growth [2]. The smaller to average pits are active when compared to larger pits which are fewer in number. These small to average pits helps in formation of a crack which would propagate deep through the material [31] as shown in Figure 2.3.

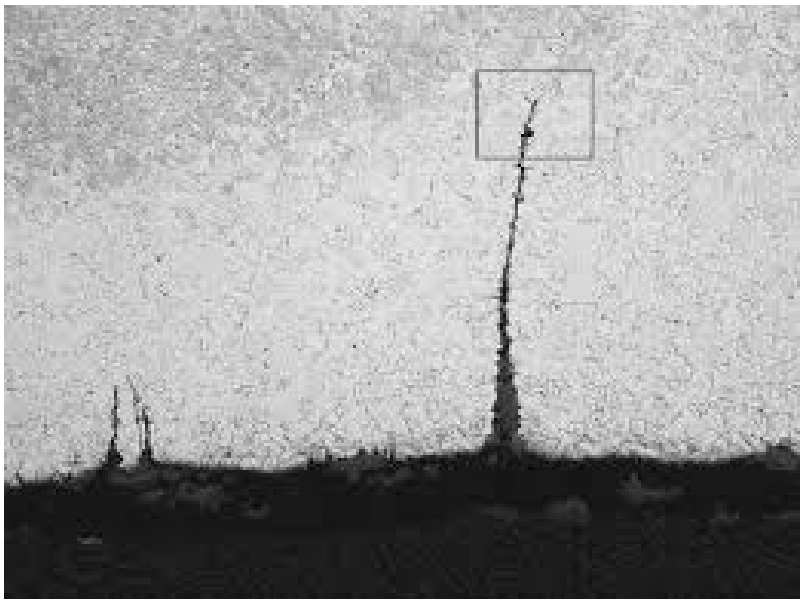

Figure 2.3: Narrow and deeper cracks [31].

The development of pits to crack growth due to fatigue is related to shape factor, and at higher aspect ratio fatigue cracks that are deeper and narrow are formed rather than wider cracks [31]. These formed pits are anisotropic in nature and the size is larger at the grains in the direction of propagation, which shows that the pit grow along the surface of the metal due to cyclic fatigue that enhance to the propagation of cracks [30].

2.4 Effects of Corrosion on Fatigue Life

Mechanical variables and mechanical driving forces are factors that should be considered for effects of corrosion fatigue. The variables such as conductivity, temperature and other sources are responsible for the metal to get damaged. Firstly the formation of crack is a complex process that can result from the formation of pits, electrochemical reaction conditions including the role of strain in creating crevices. Secondly corrosion fatigue is also dependent on time factor. Therefore, slow rate of loading causes more

damage than higher loading rates. Increasing the strain rate at cracks starting point can cause a detrimental effect on the design life period by enhancing electrochemical reactions. One of the prominent factors is an electrochemical environment that influences to cyclic deformation of the structure. Loops that are caused due to high temperatures and water under inactive environmental conditions affect the relation between stresses and strains causing elastic and plastic deformation and hence lead to micro cracking [34]. Very low values of stress failures and very short failure timing can be absorbed in a corrosive environment, as shown in Figure 2.4, compared to noncorrosive environment.

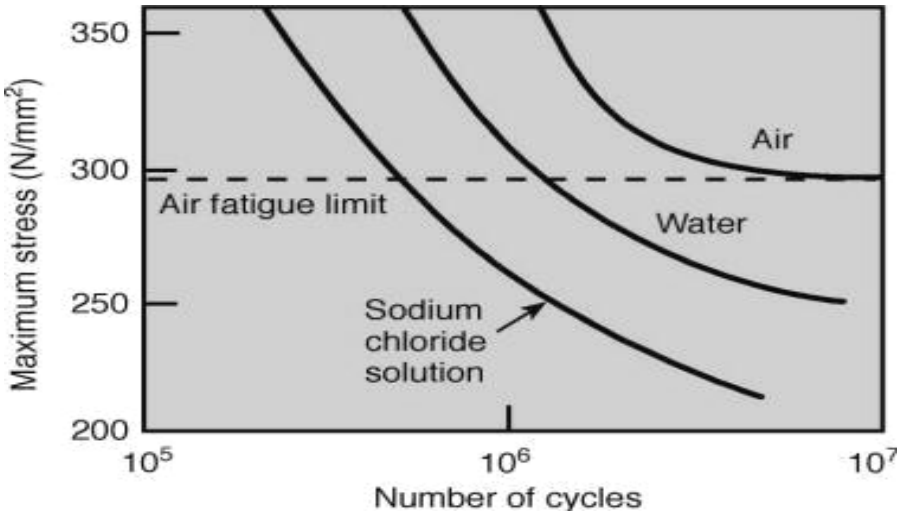

Figure 2.4: Number of cycles vs. stresses [34].

To estimate the life of the structure with the existence of crevices, the loading and experiment is carried out even in presence of the crevice. The formation of the pit under the surface, the shape and cross section of the pit/hole is difficult to determine the value of stress intensity factor. Unless failure occurs, these two factors, the stress intensity and change in stress intensity cannot be determined. On inspection of the initial corrosion crack the values can be obtained and this helps in improving fatigue life. Fatigue corrosion failure

can be prevented from minimizing cyclic stresses, reducing and distributing stresses, change in design, avoiding internal stresses, more resistive material should be used; a corrosive free environment would be of great prominence [4, 16].

2.5 Fracture Mechanics

Fracture mechanics is the study of the propagation of cracks through a material [2]. This field uses solid mechanics to determine the crack growth through the relationship between an applied load and the material's resistance to fracture. Crack propagation is broken down into three different modes. Mode I is known as the opening mode and it is a result of a force normal to the direction of crack growth. Mode II is known as the sliding mode and it is caused by an in-plane shear stress. Mode III is known as the tearing mode and it is a result of out of plane shear stress [2]. Fig. 2.5 illustrates all three modes and the forces which cause them. Since the current research involves tensile testing, mode I is the mode of primary concern.

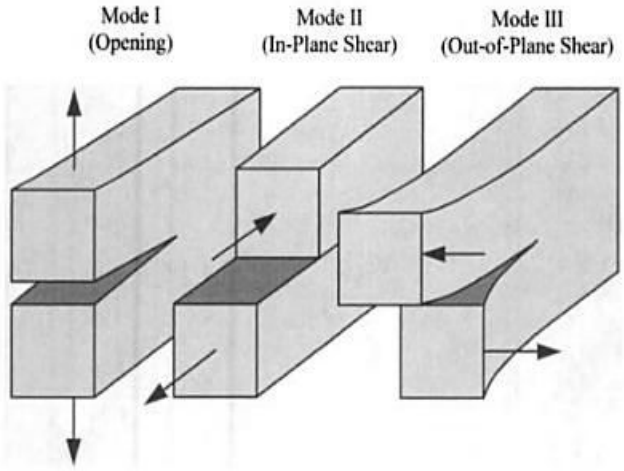

Figure 2.5: The three modes shapes referred to in fracture mechanics. Mode I is the mode of concern for the current research [2].

For each of these modes, the effect on an applied force on crack growth has a unique relationship. For mode I, the primary measure of the effect of the load on crack growth is known as a stress intensity factor K_I, Equation 2.4, where σ is the applied stress and ' a' is the crack length.

$$K_I = \sigma * \sqrt{\pi * a} \tag{2.4}$$

This stress intensity factor accounts for the flaw in a given specimen, in this case 'a' crack, will continue to grow as well. In the case of cyclical loading, the stress intensity factor is modified to account for the maximum and minimum stresses. The range of the stress intensity factor ΔK, Equation 2.5, is used in the Paris law [8].

$$\Delta K = K_{max} - K_{min} \tag{2.5}$$

Also, Equation 2.6, to define the rate of the crack growth as a function of the stress intensity factor ΔK. Material constants are denoted by m and C. As Paris law states, as the stress intensity factor increases the growth rate of crack also increases.

$$\frac{da}{dN} = C * \Delta K^m \tag{2.6}$$

Figure 2.6, illustrate three regions or three modes are observed. At low levels of stress intensity represented as region 1, the crack growth rate is rapid and sensitive to stress intensity within the region, a value where the stress corrosion crack growth rate is very low

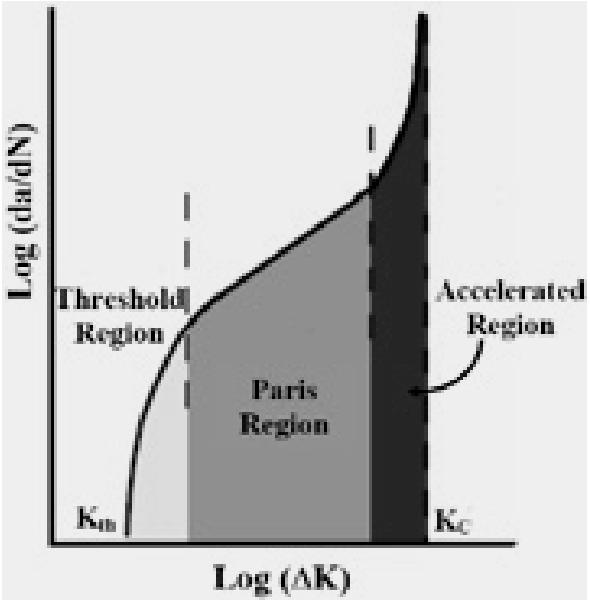

Figure 2.6: Typical fatigue crack growth behavior in metals [9].

pointed or determined and this value may also be zero. The second region represented the rate of crack growth depends on factors like temperature and properties such as viscosity [2].

2.6 Previous Research

Pitting and fatigue have always been interest of research in the recent past. The foundation step for this area of research has been laid by McEvily and Paris; they concentrated on the growth of cracks and their mechanism and led to the fundamentals of fracture mechanics. The research conducted by them helped a lot in studying how corrosion pit leads to the initiation of crack and the growth of crack rates, influence of stresses induced due to cyclic loading [18, 21]. The stress intensity factor and time factor explained by Paris is highly preferred to predict the results of a specimen. In recent times an intensive research was conducted at the microscopic level in order to evaluate the proposed

mathematical concepts. Forman's research on 7075-T6 under uni-axial cyclic loading, resulted in flaws that had an effect of fatigue nature and he couldn't measure these flaws that affected the metal's fatigue behavior [9]. Wright and White idealized a conceptual study in which loading amplitude is varied in order to produce marker bands from and examined with the use of electron scanning microscope [37]. Similar type of research with the help of marker bands was conducted by Burns et al for fatigue crack growth. The rate of crack growth is compared and correlated to the values that are predicted by using the method of creating these marker bands. An investigation on pitting corrosion effect was studied by Wang but he did not apply the concepts of fracture mechanics like Forman used in his research [4, 5, 11, 36]. In addition to long crack growth research, Forman's work in the study of where and how cracks initiate in aluminum alloy specimens spawned a totally new area of research that concerned itself with the crack initiation [8, 11]. Forman's work confirmed that the stress intensity factor range was a primary factor in crack growth rate. He also determined that cracks more easily initiated from engineering defects such as scratches or nicks in the surface. He performed his experimental testing using uni-axial cyclic loading in 7075-T6 aluminum specimens in a non-corrosive environment [11].

Previous studies state that the presence of corrosive environment affects and reduces fatigue life [13, 25, 28, 38]. This type of corrosion attack may result in reducing fatigue life, so it is a significant point to account for this type of attack to predict the lifetime of the structure. Pao et al. conducted various researches and stated that the presence of corrosive environment helped in decreasing the fatigue life and decreased the crack growth initiation [28]. To explain this concept of crack formation, a study on micro crack formation under repetitive loads was conducted by Lukas [22]. This research stated that a noticeable effect

in initiation of fatigue growth due to this micro cracks, but was not able to explain a method for determining these phenomena. The formation of cracks often initiated from the pits on specimens. For the specimens without corrosion pits there was no particular region from which such a crack developed [22]. Later Burns developed a method to determine this phenomenon of the initiation of crack [5]. The surface near the pits, in which initiation of crack took place, had a significant influence on crack initiation behavior.

Various studies on development of pit to crack using fracture mechanics were conducted in laboratories and did not have any corrosive environment. Lee conducted some tests to examine the fatigue life under the influence of pre-existing corrosion pits in 2024-T3 and found that crack initiated from corrosion pit [19]. However, he focused on pre-existing corrosion specimens from saltwater. After analysis he concluded that fatigue life of 2024-T3 was reduced due to the presence of pitting corrosion and post fracture analysis helped to identify nucleation of crack, and variation of fatigue life was correlated with crack nuclei size variation [19]. There have been several studies on the transition from pit to crack done experimentally under laboratory air and corrosive environments. Air Force Institute of Technology (AFIT) also conducted some fatigue tests. Misak et al. conducted a research on fatigue crack growth uni-axial loading condition on 2024-T3 aluminum alloy [25]. Also, they developed finite element models to predict the stress intensity factor for a circular hole with a machined notch [25].

Lee and Dorman studied the fatigue of specimens of aluminum alloy in corrosive environment [20]. The study did not use the concept of fracture mechanics and did not try to calibrate the crack growth rate during the transition of crack from corrosion pit. The

result of this study is explained in Table 2.1 in terms of aspect ratio, pit radius, and the number of cycles [20].

Table 2.1 Results from a study by Lee and Dorman [20].

Environment	Frequency (Hz)	Pit Radius (mm)	Initial Pit Aspect Ratio	Final Crack Aspect Ratio	Cycles to Detect Crack Propagation
Dry N_2	20	0.17	1.62	1.26	30,000
90-95 % RH N_2	20	0.22	0.92	1.18	35,000
0.06 M NaCl	20	0.29	1.26	1.35	45,000
0.06 M NaCl	20	0.24	0.86	1.20	85,000
0.06 M NaCl	0.1	0.29	0.67	1.28	10,000
0.06 M NaCl	0.1	0.27	2.53	1.39	51,000
Pure H_2O	0.1	0.25	0.93	1.39	40,000 (at 5 Hz)
Pure H_2O	0.1	0.23	1.86	1.03	40,000

Moreover, there has also been many researches and experiments in the field of stress concentration factors and stress intensity factors, and for a wide range of shapes. There already exists a solution for calculating the stress intensity factor of a circular hole with one radial crack at the hole boundary in an infinite plane.

In addition to all these, Hunt did a research on fatigue crack initiation and growth from two types corrosion pits at a circular hole in a 7075-T6 aluminum alloy subjected to uniaxial loads with stress ratio of R = 0.5 in both air and saltwater environments [14]. His work used a fracture mechanics approach to explore the transition from corrosion pit to crack growth. This research showed that corner-pit specimens initially have a smaller crack growth rate than through pit specimens due to the propagation of a quarter-circular crack front through the thickness of the sample [14].

2.7 Purpose of Research

The purpose of this research is to determine the crack initiation and growth behavior from a corrosion pit on the edge of a hole in 2024-T3, which is a common aircraft grade aluminum alloy. The following list provides some of the considerations of this research:

- Study crack formation from through and corner pit.
- Use concept of fracture mechanics in this study.
- Study crack initiation in ambient air and saltwater environments.
- Calculate stress intensity factors for through and corner pits.
- Make a comparison with previous studies.

2.8 Approach

In this thesis, the crack initiation and growth behavior from a corrosion pit that is electrochemically created at the edge of a hole on the specimen machined from 2024-T3 aluminum alloy are determined. In the specimens two types of corrosion pits are made, corner pit and through pit, dissimilarity among these two is explained in this thesis. The primary outcome of this thesis is to study the relationship between crack initiation duration with stress intensity factor of the specimens with through and corner pits after being exposed to air and saltwater environment respectively. Also, an approach to determine stress intensity factor was used for the hole with corrosion pit and a thin plate with crack in finite element analysis software, Abaqus. This approach is adapted as there are neither closed form solutions nor accepted models of the previously mentioned shape of specimens. Secondly the goal of this thesis is to determine the crack growth rate with respect to stress intensity factor for the specimens. Each test was done using cyclic loading in order to

replicate a fatigue environment. Fracture mechanics concept is used for this research for explanation the results. Likewise, there is presently no model for establishing the stress intensity factor for specimens with a crack from a corrosion pit. This method of developing a finite element model and then correlating this model to experimental testing by using fracture mechanics will give accurate, useful, and consistent results which will help to extend the life of the Air Force's aging fleet.

3. Methodology

3.1 Material

In this research 2024-T3 aluminum alloy is used. It is a commonly used aircraft structure material. Tables 3.1 and 3.2 show the chemical composition and the material mechanical properties.

Table 3.1: Component materials of a typical sample of 2024-T3 aluminum alloy [35].

Element	**%component**
Aluminum, Al	90.7-94.7
Chromium, Cr	Max 0.1
Copper, Cu	3.8-4.9
Iron, Fe	Max 0.50
Magnesium, Mg	1.2-1.8
Manganese, Mn	0.3-0.9
Other, each	Max 0.05
Other, total	Max 0.15
Silicon, Si	Max0.5
Titanium, Ti	Max 0.15
Zinc, Zn	Max0.25

Table 3.2: Mechanical properties of a typical sample of 2024-T3 aluminum alloy [35].

Material Property	**Value**
Ultimate Strength	483MPa
Yield Strength	345 MPa
Young's Modulus	73 GPa
Shear Modulus	28 GPa
Poisson's Ratio	0.3

The corrosion fatigue resistance of aluminum alloys varies greatly. 2024-T3 has a high ultimate yield strength, which is considered very high aluminum alloy strength for use in high stress applications. Therefore, this is one of the most common used alloys in the aircraft structures, with its high strength and excellent fatigue resistance.

3.2 Test Specimens

Figure 3.1 shows the dimensions for the uni- axial specimens. Each specimen is cut from 2024-T3 rolled aluminum sheets using of a high-pressure water jet in the AFIT machine shop. After machining the specimen, the surfaces surrounding the hole on both sides were polished using 1000 grit sandpaper. The polishing allowed to have a clean surface before chemical reaction. After polishing an electrochemical corrosion procedure was followed [28]. The procedure begins with the corners of the holes' bore being filleted with a razor-sharp blade. The radius of the fillet was approximately 0.2 mm. The fillet radius was checked with a magnifying lens to ensure the correct size. The radius is necessary because without it, the E-470 electroplating tape would not adhere well to the corner of the bore because of the 90 degree angle. The electroplating tape was used to create the shape of the corrosion pit. The electroplating tape serves as a shield against the electrochemical corrosion / etching. All surfaces that would be in contact with the tape were cleaned with isopropyl alcohol to ensure strong adhesion.

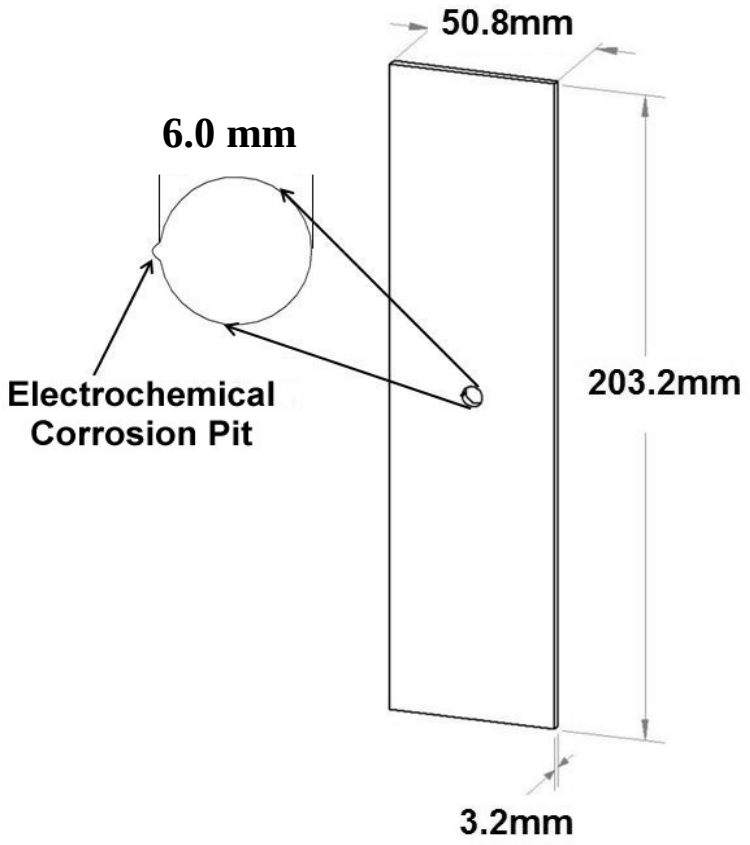

Figure 3.1: Diagram of test specimen.

Each type of pit required different taping configurations. The through pit shape was created by placing two 2.0 mm wide strips of tape approximately 0.25 mm apart on the edge of the hole perpendicular to the loading direction. The corner pits shape was created by placing a single 2.0 mm wide strip of tape with a 0.21 mm hole drilled in the center over the edge of the hole perpendicular to the loading direction. The hole was aligned so that it was centered over the edge and was bounded by the front face and the bore of the hole [14]. An example of both tape scenarios is shown in Figure. 3.2.

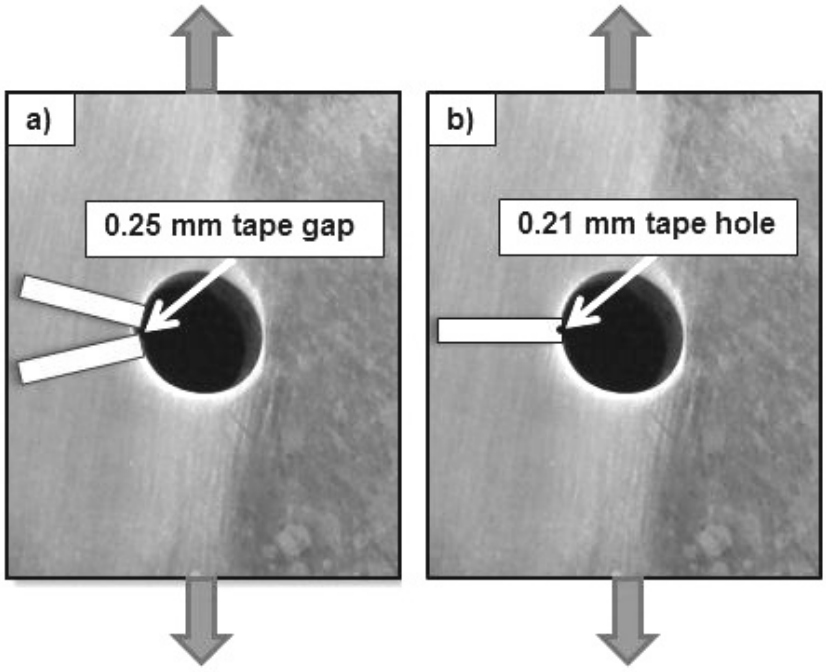

Figure 3.2: a) Tape configuration for through pit etching. b) Tape configuration for corner pit etching. Black arrows show the loading direction for each specimen [14].

Once the tape was applied, the areas in which corrosion was not needed were coated with XP 2000 Stop-off lacquer. The lacquer was applied in a circular shape with a radius of approximately 2 cm around the hole in a single coat and allowed to dry for 12 hours. Once the lacquer cured, a small plastic cylinder was attached and secured to one side of the painted region using silicone caulking. The attached plastic cylinder acted as a container for the corrosive solution in order to protect the rest of surface area from the chemical reaction. The caulking was used to both seal and secure the plastic cylinder to the painted region in order to prevent the container from leaking. To prevent any of the solution from leaving through the hole, a 2.5 cm piece of tape was applied to the side of the hole that was opposite the lacquer coating. As a result, the only areas exposed to the corrosive solution were the areas that would be investigated and named as the corrosion pits. The caulking was allowed

to cure for 12 hours before completing the reaction. A solution of 0.1MAlCl3 + 0.86MNaCl + HCl (pH =2) was used to corrode the aluminum specimen [14]. The chemical reaction was driven by a power supply. The positive output lead was clipped to the non-coated portion of the specimen, and the negative output lead was clipped to a platinum electrode that was submerged in the corrosive solution. During the reaction, hydrogen bubbles would form over the corrosion site and act as an insulator; ultimately stifling or stopping the reaction. A small brush or pipette was used to circulate the solution in the chamber and to remove the bubbles so that the reaction could continue at a satisfactory rate. After approximately 9-15 minutes, the corrosion pit reached the desired size and the reaction was terminated [14]. The solution was removed using a glass pipette. The plastic cylinder, lacquer, and tape were also removed from the specimen to expose the newly formed corrosion pit.

Figures 3.3 and 3.4 show the two types of pits formed during the reaction. The specimen was then rinsed with water and dried thoroughly. The corrosion pits were measured using the Zeiss optical microscope. The measured pit sizes were used in the calculations to approximate the stress intensity ranges for each specimen. The initial pit size and the approximated stress intensity ranges for each specimen are shown in Table 3.3.

The specimens were labeled with a three letter code. The first letter (2) refers to the current set of specimens. The second letter refers to either air (A) or salt (S) environments. Finally, the third letter refers to the type of pit; either through pit (l) or corner pit (S).

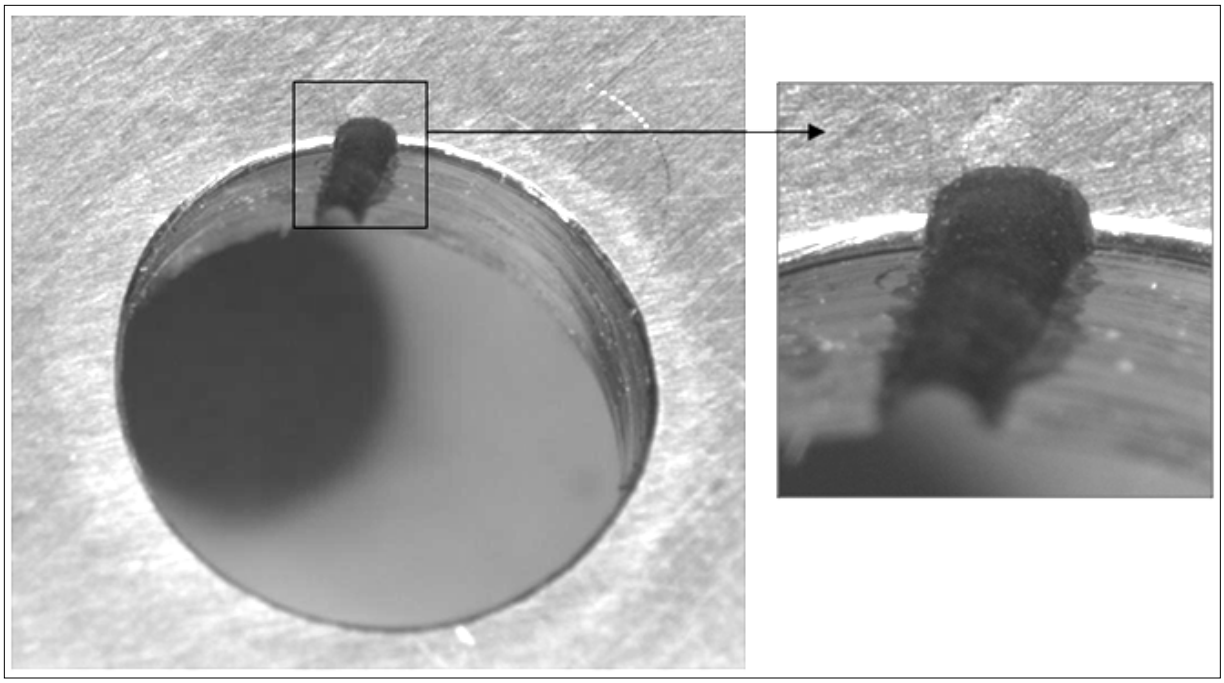

Figure 3.3: Example of through corrosion pit.

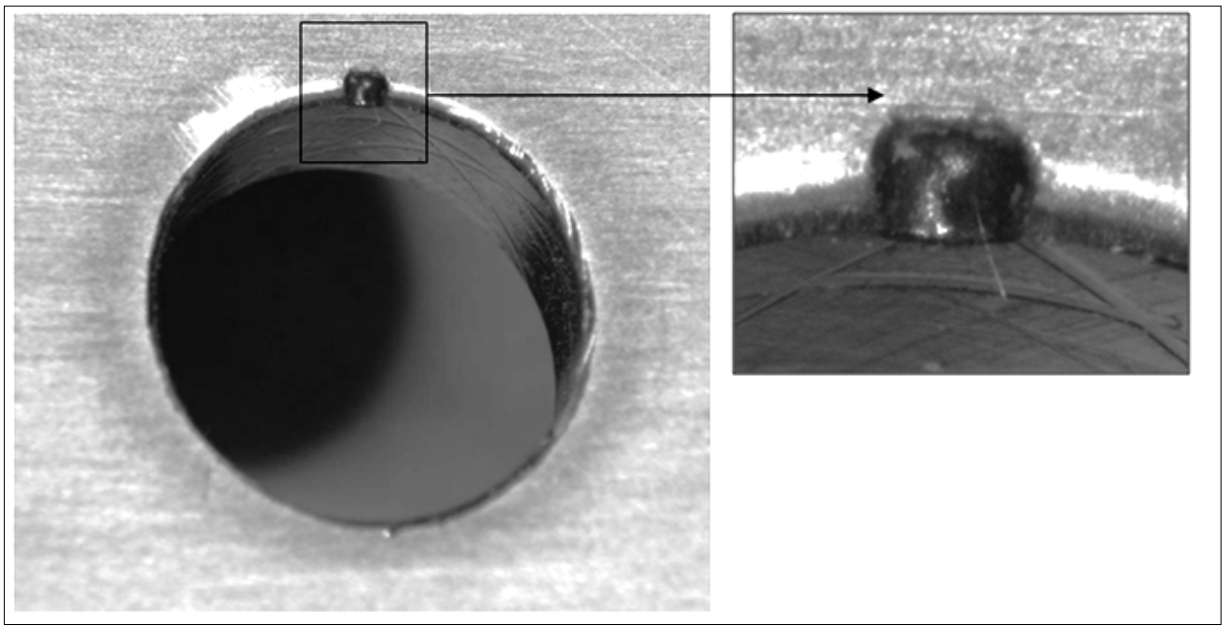

Figure 3.4: Example of corner corrosion pit.

Table 3.3: Details of test specimens.

Specimen	Pit Radius (mm)	Pit Type	Environment	ΔK (MPa√m)
2AI-01	0.5	Through	Air	5.06
2AI-02	0.30	Through	Air	6.08
2AI-03	0.30	Through	Air	3.12
2AI-04	0.28	Through	Air	4.19
2AS-01	0.51	Corner	Air	3.89
2AS-02	0.46	Corner	Air	4.60
2AS-03	0.35	Corner	Air	3.43
2AS-04	0.54	Corner	Air	2.31
2SI-01	0.44	Through	Saltwater	5.40
2SI-02	0.50	Through	Saltwater	3.00
2SI-03	0.38	Through	Saltwater	3.75
2SI-04	0.45	Through	Saltwater	3.47
2SS-01	0.45	Corner	Saltwater	2.47
2SS-02	0.34	Corner	Saltwater	4.03
2SS-03	0.38	Corner	Saltwater	1.98
2SS-04	0.50	Corner	Saltwater	2.98

* Initial ΔK values were calculated by FEA.

3.3 Test Procedures

After preparing the specimens, they were tested under cyclical uniaxial loading with stress ratio of 0.5 in a material testing system machine, MTS. Fatigue tests were conducted until either crack initiated and grew to a length of 17 mm or 1 million cycles without crack initiation.

Initially, the experimental applied loads were calculated using closed form solutions from a book written by Dowling shown in Equation 3.1, where a is the crack length, c is radius of the hole, w is the width of the specimen, F_{min} and F_{max} are the minimum and

maximum applied loads respectively, and ΔK_I is the stress intensity range for mode I loading [8]. This equation used the crack length, other geometric properties and applied loads to calculate the approximate stress intensity factor for a through crack originating from a circular hole with a radial circular pit.

$$\Delta K_I = 0.5 \cdot \left(3 - \frac{a}{c+a}\right) \cdot \left(1 + 1.243\left(1 - \left(\frac{a}{c+a}\right)\right)^3\right) \frac{F_{\max}\left(1 - \frac{F_{\min}}{F_{\max}}\right)}{wt} \cdot \sqrt{\pi a} \qquad (3.1)$$

This equation was used to calculate the stress intensity factor for the geometry of current experiment. The equation was thought to be accurate enough to give approximate values used in the calculation of future experimental methods. The results from the equation and the ones calculated by means of the finite element analysis (FEA) are slightly different. These results are discussed in the Finite Element Analysis section of this thesis. After the tests the values from the FEA was used in the analysis of the tests.

Figure 3.5 shows the test machine that was used in this research. This machine has three main part, load frame, camera, and software program. Software program can communicate with the load frame in order to get a required data from experiment testing. Also, MTS controls the loading situation where the crack growth must be monitored through external equipment. Result of the crack growth is small; therefore, a high fidelity and high magnification camera was a perfect fit.

Figure 3.5: The floor-standing 810 mechanical testing system (MTS) [27].

In order to measure the crack growth as the number of cycles progressed, a Pixelink camera and software package were used to photograph and measure a crack length. Figure 3.6 shows the test setup of the camera and the specimen in the grips of the MTS machine. The Pixelink software uses the pixels in the image to calculate a length of an object in the image. Calibration of the software and machine was set up in front of the camera so that the specimen was in focus and a picture of the hole was taken. By means of this the dimensions of the hole could be verified by the optical method.

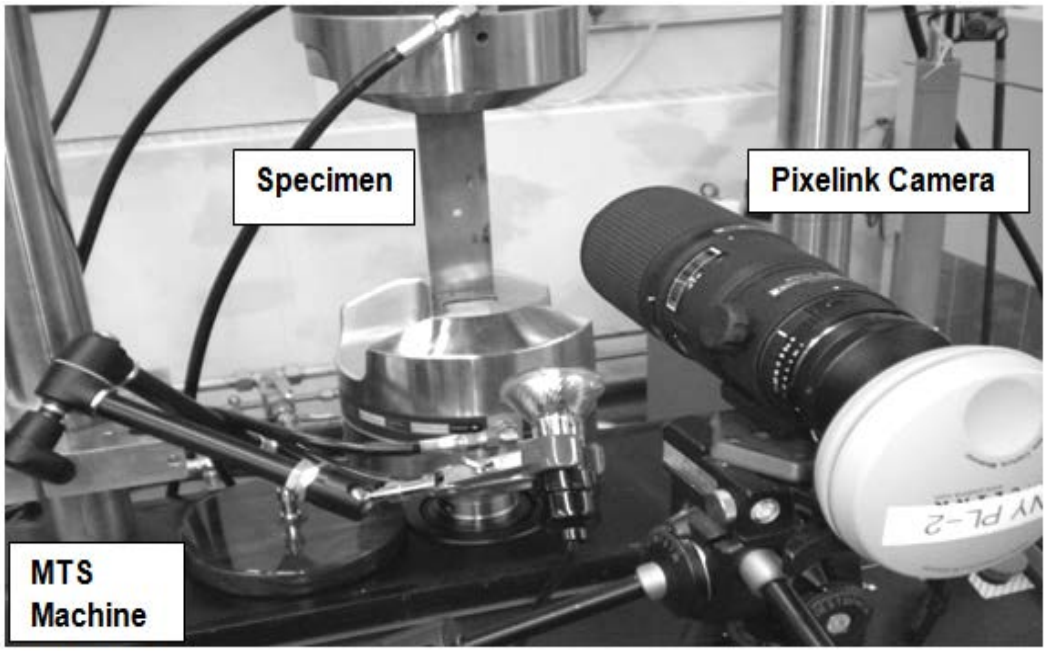

Figure 3.6: The test setup.

Then the software was calibrated so that the number of pixels across the diameter of the hole corresponded to the actual length of the hole. Particular attention was paid to the stability of the camera, care was taken so that the camera was not moved in anyway during the testing. During the testing the camera was not to be disturbed. Additionally, the camera and software were re-calibrated when a new specimen was tested. Furthermore, an incandescent light bulb was used to provide light for the picture where the angle of the light hit the surface of the specimen to expose cracks in their infancy. It is impossible to see the cracks until they reached a significant length if an incorrect lighting is used. Figure 3.7 shows a chamber with saltwater (3.5% NaCl) installed on the specimen.

Figure 3.7: A chamber with salt water installed on the specimen.

When the crack reached a length of approximately 17 mm as shown in Figure 3.8, the test was stopped and the specimen was considered to have failed. This was done to preserve the fracture surfaces.

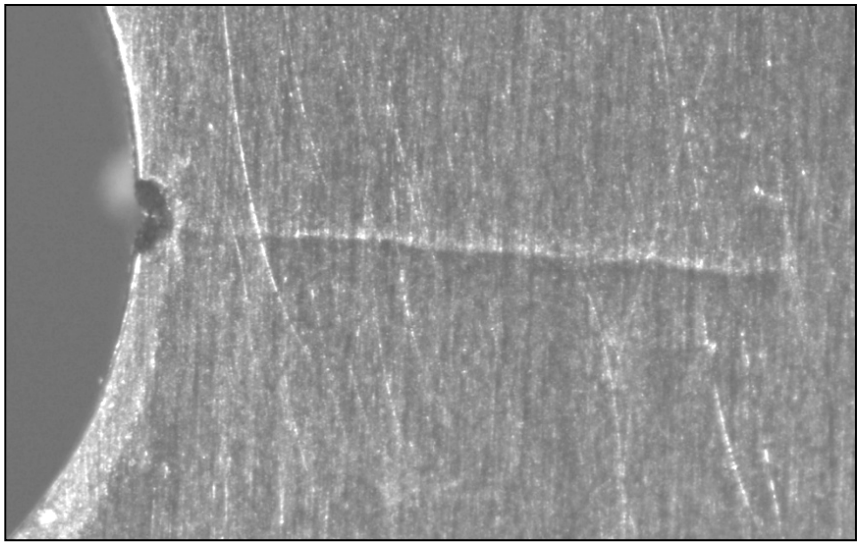

Figure 3.8: Crack propagation for uniaxial loading.

3.4 Finite Element Modeling

As discussed in Section 3.3, there is a closed form solution for calculating the stress intensity factor of a crack that originates from a hole in a flat plate as given in Equation 3.1. To determine if this equation could be used to approximate the stress intensity factor of the test specimens, the specimens were analyzed by Abaqus, which is a finite element analysis (FEA) code. Abaqus requires a number of assumptions to be declared by the user. The author assumed the following throughout the modeling procedures [14]:

- The aluminum material was isotropic and homogeneous.
- The mechanical properties of the aluminum alloy were constant (E=73 GPa, ν=0.33).
- The pits are a uniform shape with smooth edges and no irregularities.
- There were no other flaws of any kind in the specimens and the crack initiated from the corrosion pit.
- The applied load was completely perpendicular to the crack growth direction.
- There is no variation in the applied loads [14].

The test consisted of loading the specimen in tension in the longitudinal direction to determine the stress concentration factor caused by the hole [14]. After refining the mesh elements in finite element analysis, the values from Abaqus matched within 10% of the calculated values from Dowling Equation 3.1 as shown in Table 3.4. The final meshed models are shown in Appendix A. Moreover the mesh is more refined near the hole compared to the other area of the model. Global mesh of a uni-axial specimen is shown in Figure 3.9.

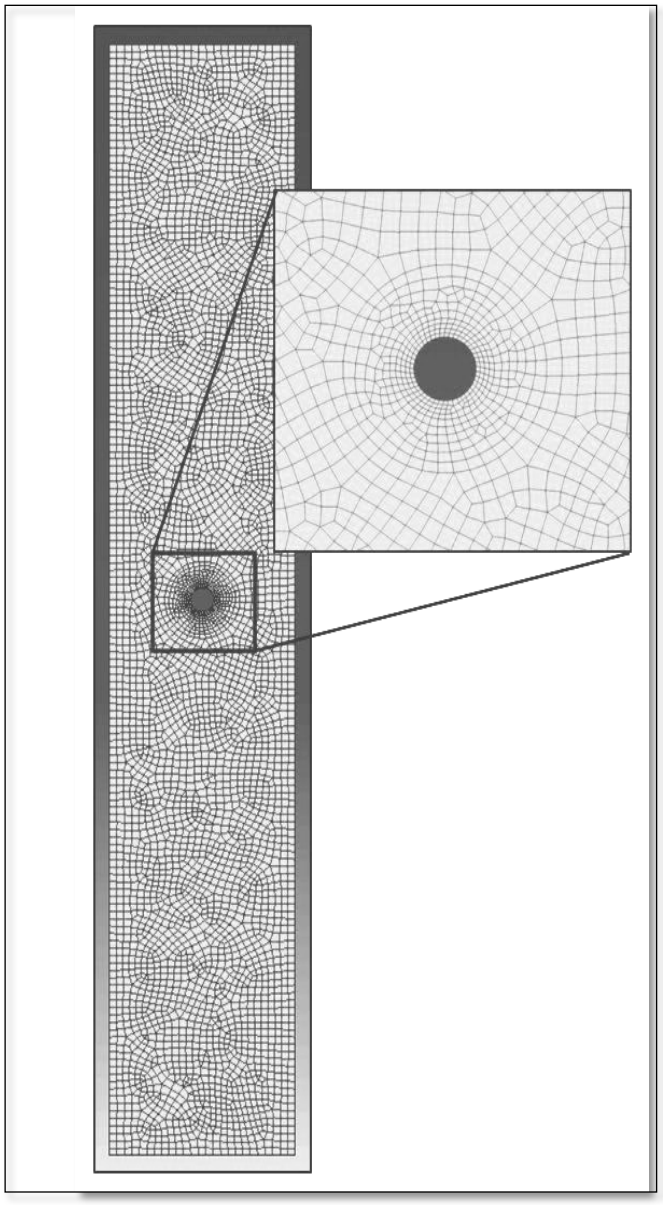

Figure 3.9: Global mesh of uniaxial specimen.

Figures 3.10 and 3.11 show the global and the refined meshes of the specimens with the crack length of 0.25 mm and 15 mm. This mesh is more refined near the crack tip when compared with the other location of the specimen. Therefore, accurate stress intensity factor values will be achieved.

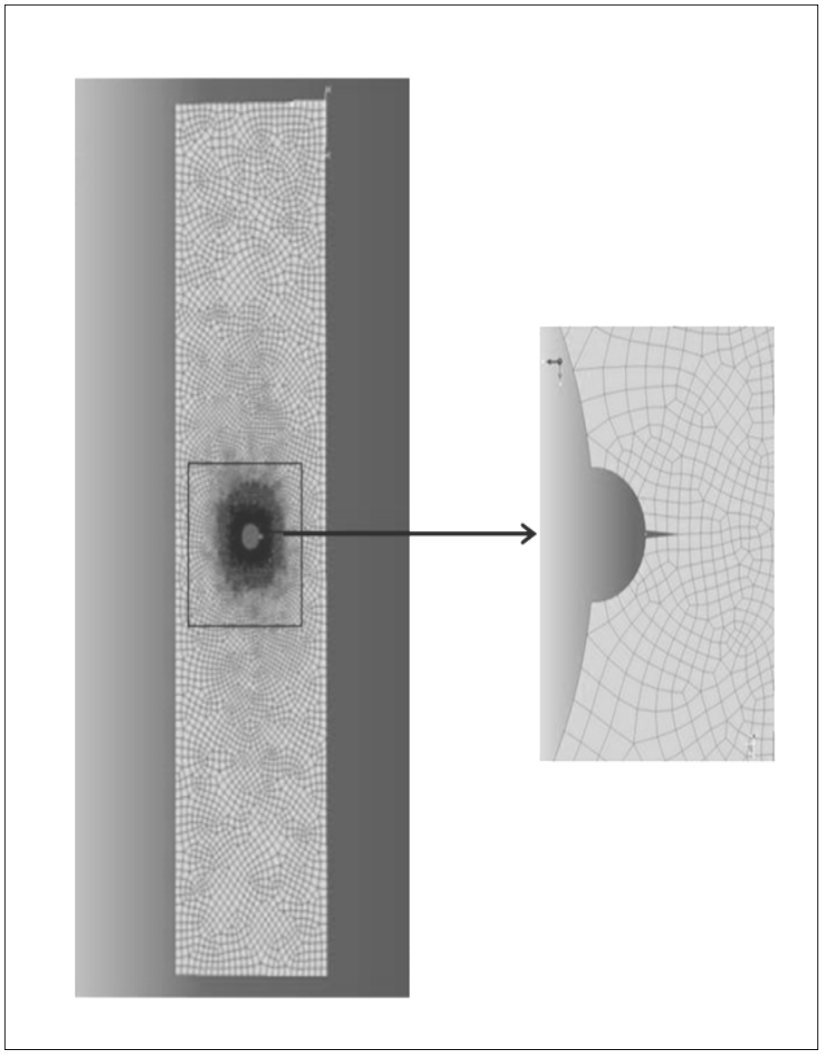

Figure 3.10: Global mesh of uniaxial specimen with a refined mesh around corrosion pit with a crack length of 0.25 mm.

The next step is to develop a finite element model to confirm results from the closed form solution provided by a horizontal crack from the edge of the hole. The same refinement procedures were used as in the stress concentration factor scenario and final mesh is shown in Figures A.3.

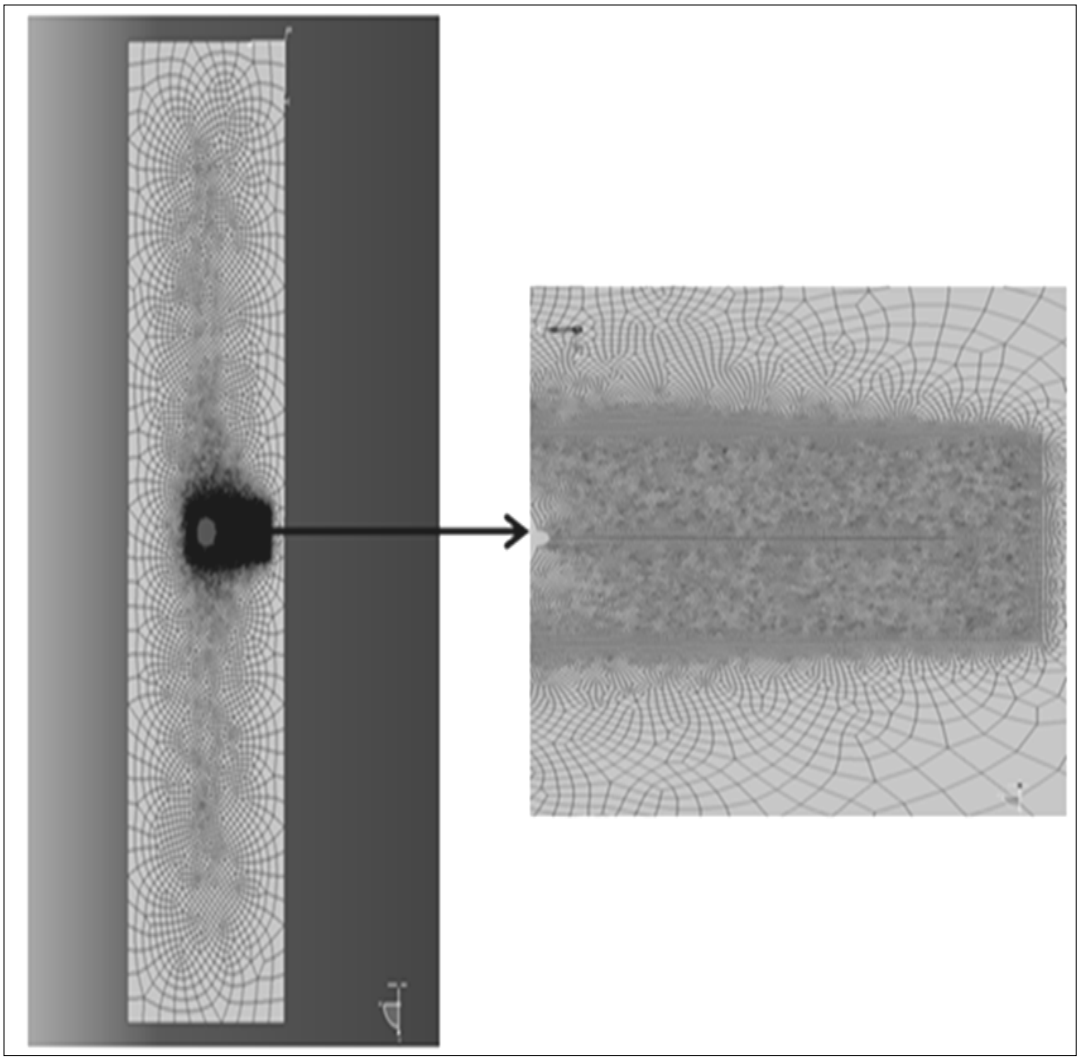

Figure 3.11: Global mesh of uniaxial specimen with a refined mesh around corrosion pit with a crack length of 15 mm.

The differences between the closed form and finite element solution are because of the assumptions of the equation. The closed form solution assumed an infinitely long and wide specimen. In reality, experimental specimens do not fulfill these assumptions therefore, deviation from the equation is expected. But in finite element analysis the dimensions were taken into account.

After successful completion of a two-dimensional model of a hole with a horizontal crack, the mesh and element settings were applied to another different model consisting of a crack originating from corrosion through pit on a circular hole. This second model more accurately mimicked the actual geometry of the specimens. The results for the initial ΔK for expected value of the closed form solution as well as the corresponding results of the finite element models are shown in Table 3.4.

Table 3.4: ΔK values from the closed form solution and finite element solution.

Specimen	Predicted ΔK, (MPa ∗ √m)	ΔK from Abaqus Model, (MPa ∗ √m)	Total Flaw Size (mm)
2Al-01	5.11	5.06	0.51
2Al-02	5.50	6.08	0.30
2Al-03	2.80	3.12	0.30
2Al-04	4.50	4.19	0.28
2Sl-01	5.02	5.40	0.44
2Sl-02	2.80	3.0	0.50
2Sl-03	3.30	3.75	0.38
2Sl-04	3.25	3.47	0.45

The pit diameter in the model was set and the pits were assumed smooth, i.e. uniform half-circles to reduce the complexity of the finite element model. The ΔK values predicted by Abaqus for through pit specimens for this model matched identically to the results from closed form solution.

After through pit specimens were modeled, the next step was modeling the corner pit specimens. For corner pit that requires three dimensional modeling, finite element analysis does have the ability to mesh complex shapes as shown in Figure 3.12.

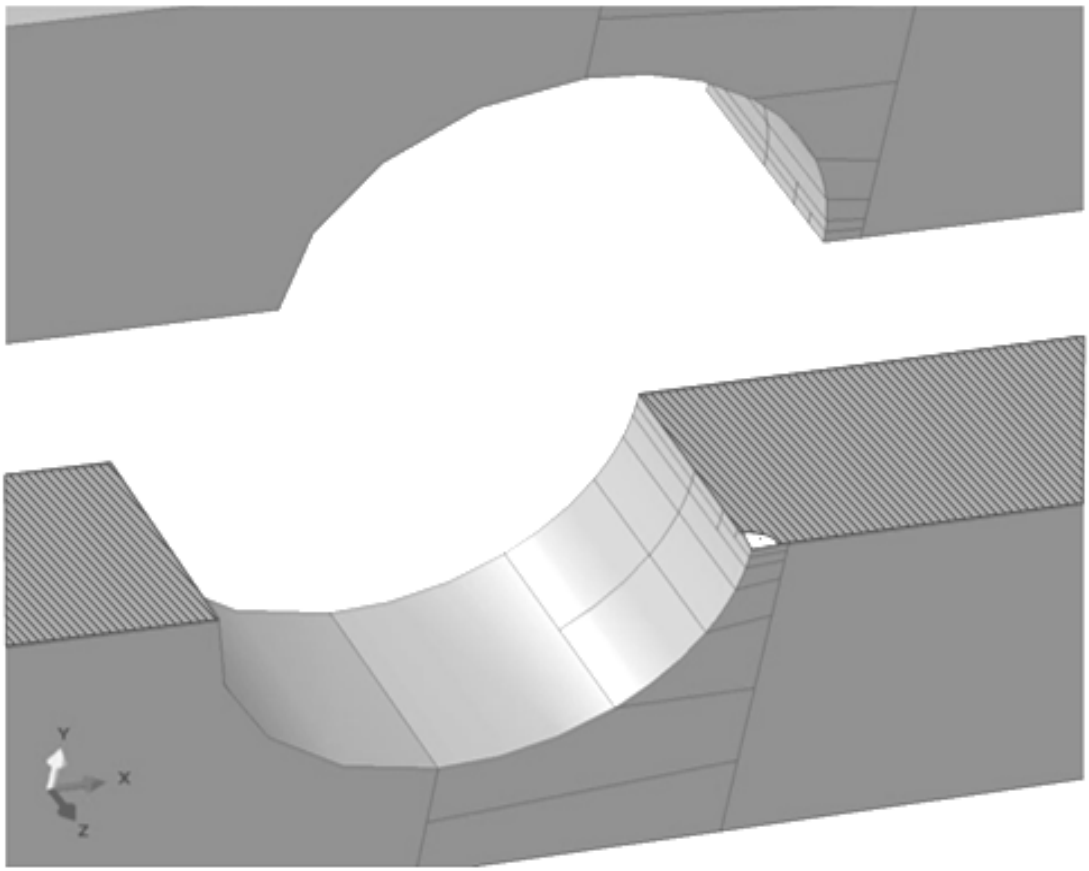

Figure 3.12: 3D model of specimen with corner pit.

4. Results and Discussion

4.1 Chapter Overview

This chapter presents the research results conducted on 2024-T3 aluminum alloy for corrosion fatigue. The uni-axial specimens with through pits are discussed in section 4.2. Section 4.3 discusses the results for uni-axial specimens with corner pits. The results are displayed in plots demonstrating the stress intensity factor range with respect to number of cycles required for fatigue crack initiation and growth. Also, the SEM images from fatigue crack initiation are discussed in section 4.4. Table 4.1 shows results from all tests.

Table 4.1: Results of all tests.

Specimen	R	Δσ MPa	radius of pit mm	N_i cycles	Initial ΔK MPa*m^1/2
2AI-01	0.5	46	0.50	640,421	5.06
2AI-02	0.5	56	0.30	120,012	6.08
2AI-03	0.5	29	0.30	1,000,000	3.12
2AI-04	0.5	41	0.28	850,000	4.19
2SI-01	0.5	49	0.44	34,506	5.40
2SI-02	0.5	29	0.50	1,000,000	3.00
2SI-03	0.5	35	0.38	220,022	3.75
2SI-04	0.5	32	0.45	408,000	3.47
2AS-01	0.5	75	0.51	45,000	4.60
2AS-02	0.5	53	0.46	290,000	3.43
2AS-03	0.5	36	0.35	1,000,000	2.30
2AS-04	0.5	60	0.54	175,000	3.89
2SS-01	0.5	38	0.45	690,000	2.47
2SS-02	0.5	56	0.34	34,506	4.03
2SS-03	0.5	31	0.38	1,000,000	1.98
2SS-04	0.5	46	0.50	240,000	2.98

* Initial ΔK values were calculated by FEA.

4.2 Through Pit Specimens

Crack initiation and growth occurred for ΔK's of 5.06, 6.08, 3.12 and 4.19 MPa*m^(1/2) when exposed to air and for ΔK's of 5.40, 3.0, 3.75, and 3.74 MPa*m^(1/2) when exposed to a saltwater environment. For the specimen with ΔK of 3.13 MPa*m^(1/2) crack did not initiate over 1 million cycles in the laboratory air environment so this particular experiment was terminated. Also in the saltwater environment the specimen with ΔK of 3.0 MPa*m^(1/2) didn't have any crack over 1 million cycles. The crack lengths versus the number of cycles curves are shown in Figures B.1, B.2, B.3, B.4, B.5, B.6, and B.7 (Appendix B). The da/dN vs. ΔK curves derived from the experimental data are shown in Figures B.8, B.9, B.10, B.1, and B.12 (Appendix B). During the tests, the crack length was measured at every 5000 load cycles. The crack length with respect to the number of cycles was plotted. Trend lines were drawn by using Excel. The trend line predicted when the crack initiated with more accuracy than the camera monitoring technique. This is because during some experiments the cracks would be unseen only until they reached approximately 1 mm. Moreover, the crack growth rate curves were developed by using the slope of the least-squares fit from the crack length vs. number of cycles plot. This was done because da/dN is by definition the rate of change of a crack length vs. cycles curve. Since the trend line of the crack length reduced some of the data scatter, the derivate of this line further reduced the data scatter that is inherent in experimental measurements. This data was used to plot the cycles until initiation vs. initial ΔK, and the crack growth rate vs. ΔK as shown in Figure. 4.1 and 4.2a, respectively.

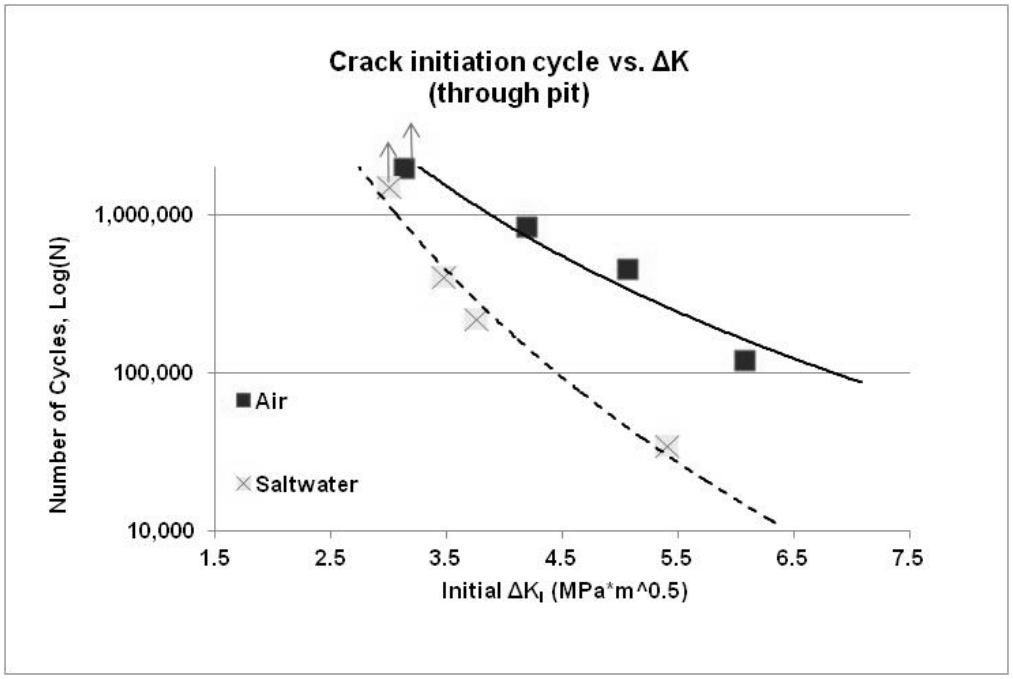

Figure 4.1: Plot of the cycles until crack initiation vs. the stress intensity factor for the through pit specimens in both air and saltwater (3.5 %) environment.

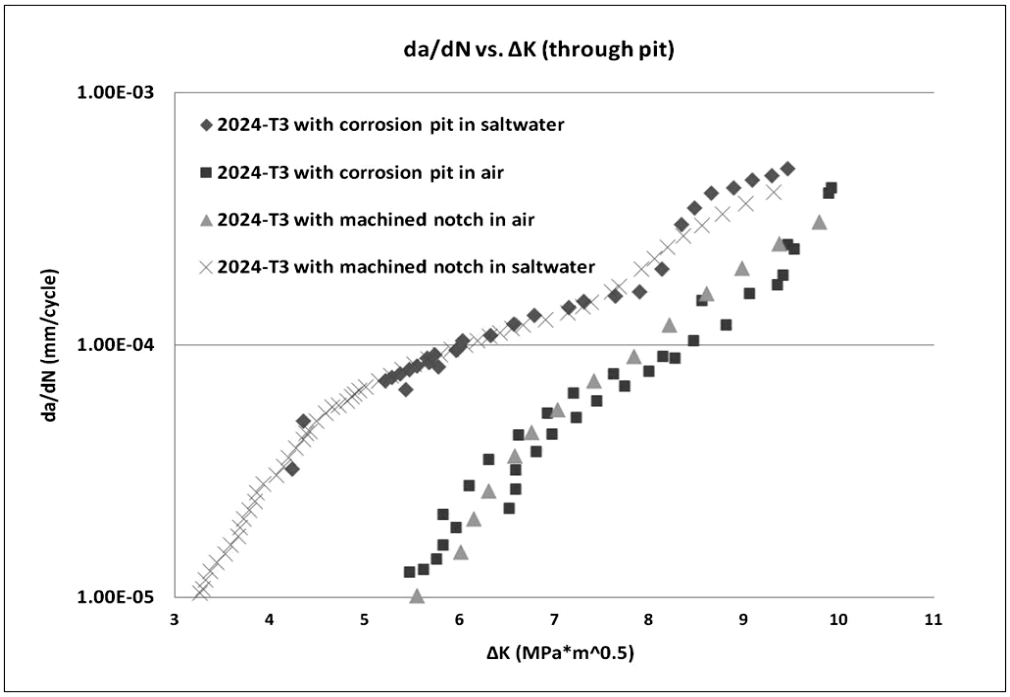

Figure 4.2a: The crack growth rate as a function of the stress intensity factor for corrosion pit and machined notch.

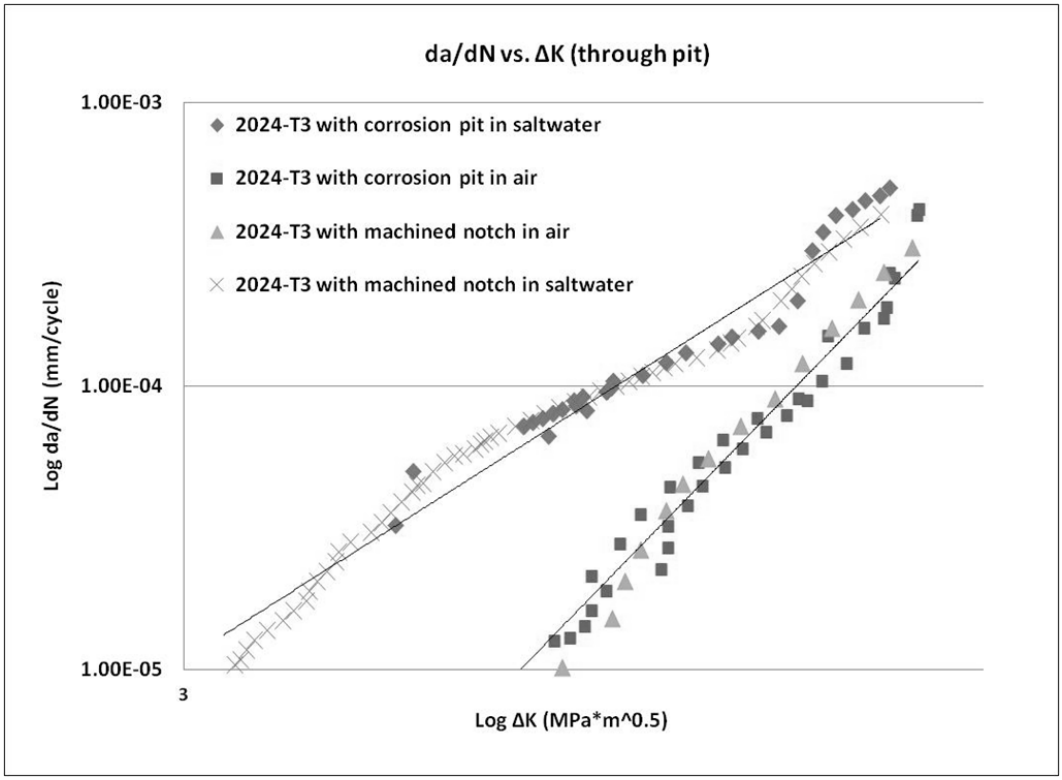

Figure 4.2b: The crack growth rate as a function of the stress intensity factor in logarithmic scale for corrosion pit and machined notch.

The crack growth rate as a function of the stress intensity factor on logarithmic scale was also drawn as shown in Figure 4.2b. By using these curves and Paris constants were determined as C= 1.316E-08, and m=4.16 for both studies.

4.3 Corner Pit Specimens

Crack initiation and growth occurred for ΔK values of 3.43, 3.89, and 4.6 MPa*m^(1/2) in air. Fatigue crack did not initiate in the specimen with ΔK value of 2.31 MPa*m^(1/2) over 1 million cycles. The crack growth plots for the specimens that did have crack growth in air are shown in Figures C.1, C.2 and C.3 (Appendix C). In the saltwater environment, crack initiated for ΔK of 2.47, 2.98, and 4.03 MPa*m^(1/2). In saltwater, for

the specimen with ΔK value of 1.98 MPa*m^(1/2) crack did not initiate over 1 million cycles so this particular test was terminated. The crack growth vs. ΔK plots are shown in Figures C.5, C.6, and C.7 (Appendix C). Additionally, the da/dN vs. ΔK plots for the specimens that had crack initiation and growth are shown in Figures C.8, C.9, C.10, C.11, C.12, and C.13 (Appendix C). Figure 4.3 shows the relation between the crack initiation vs. the stress intensity factor for corner pit tests.

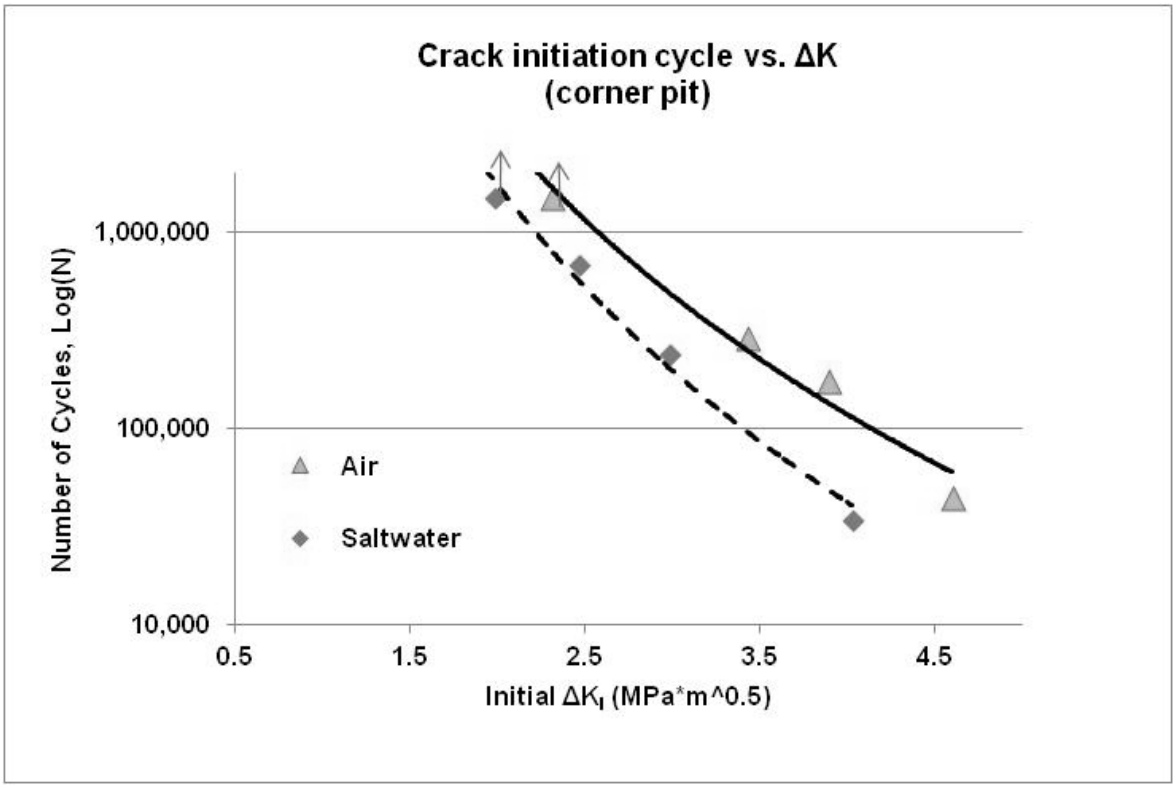

Figure 4.3: Plot of the cycles until crack initiation vs. the stress intensity range for the corner pit specimens in both air and saltwater (3.5 %) environments.

4.4 Microscopic Results

After completion of the tests, the test specimens were cut into two halves and then they were separated. Henceforth, the actual pit size could be measured with the SEM or other optical microscopes because the entire pit could be examined. Examples of both through pit and corner pit are shown in Figures 4.4 and 4.5, and the measurements are shown in Figures 4.6 and 4.7, respectively. Since the pits have non-uniform geometries, many measurements were required along the length of the pit.

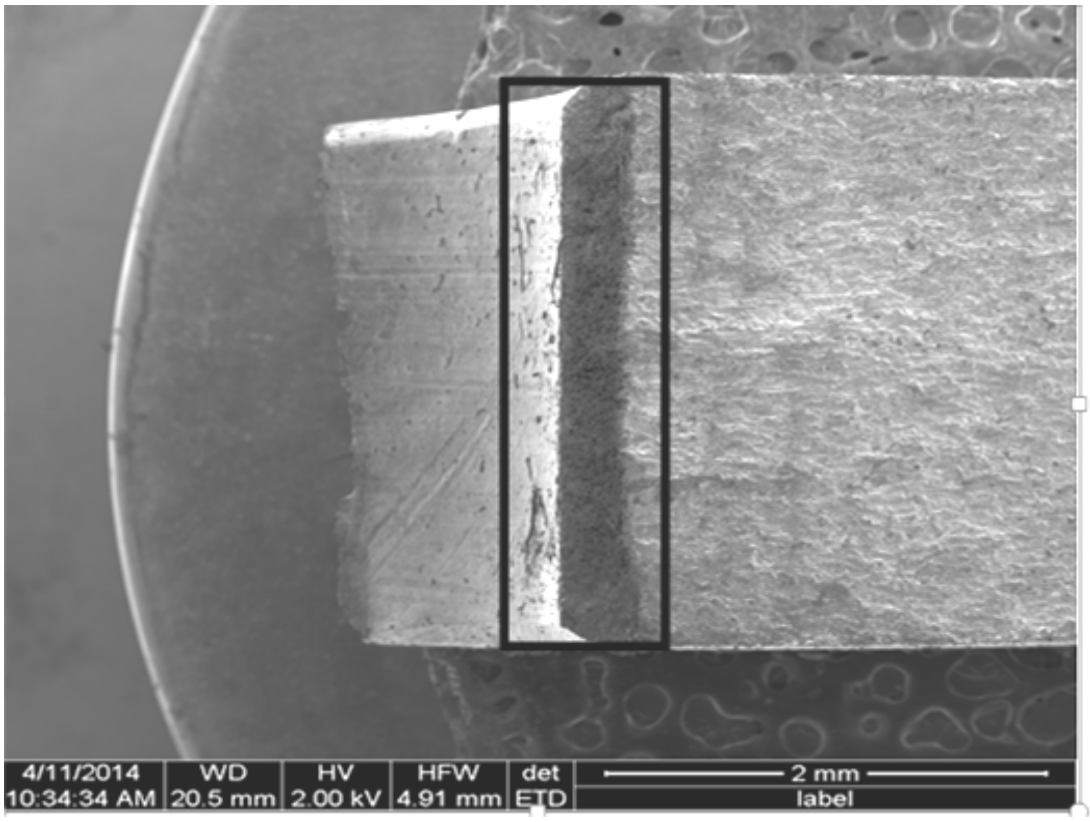

Figure 4.4: Top view of the through pit and fracture surface.

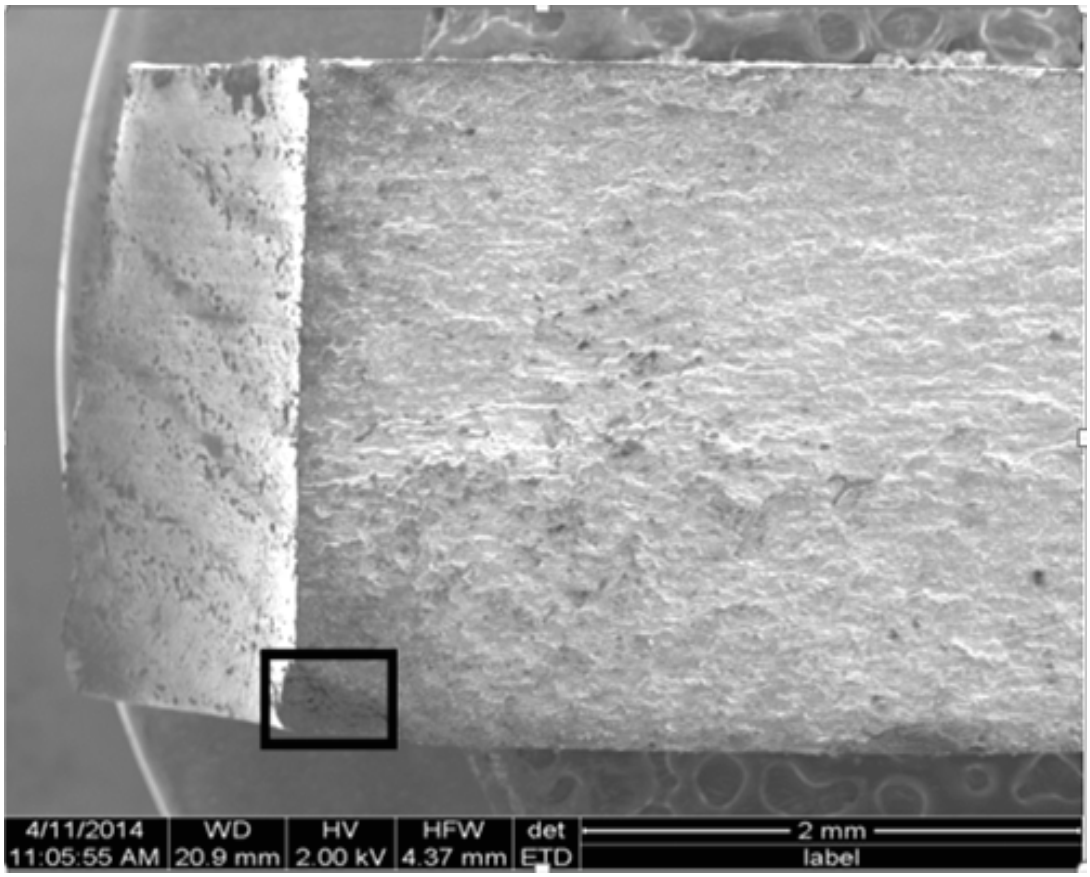

Figure 4.5: Top view of the corner pit and fracture surface.

The average pit size from each specimen was used in the corresponding Abaqus model to determine the stress intensity factor prior to any fatigue loading. Changing ΔK values allowed the values previously calculated from the closed form solution to be replaced in the various plots and tables. The microscopes were important for determining the initial conditions of the specimen and consequently, examining the way fatigue cracks started.

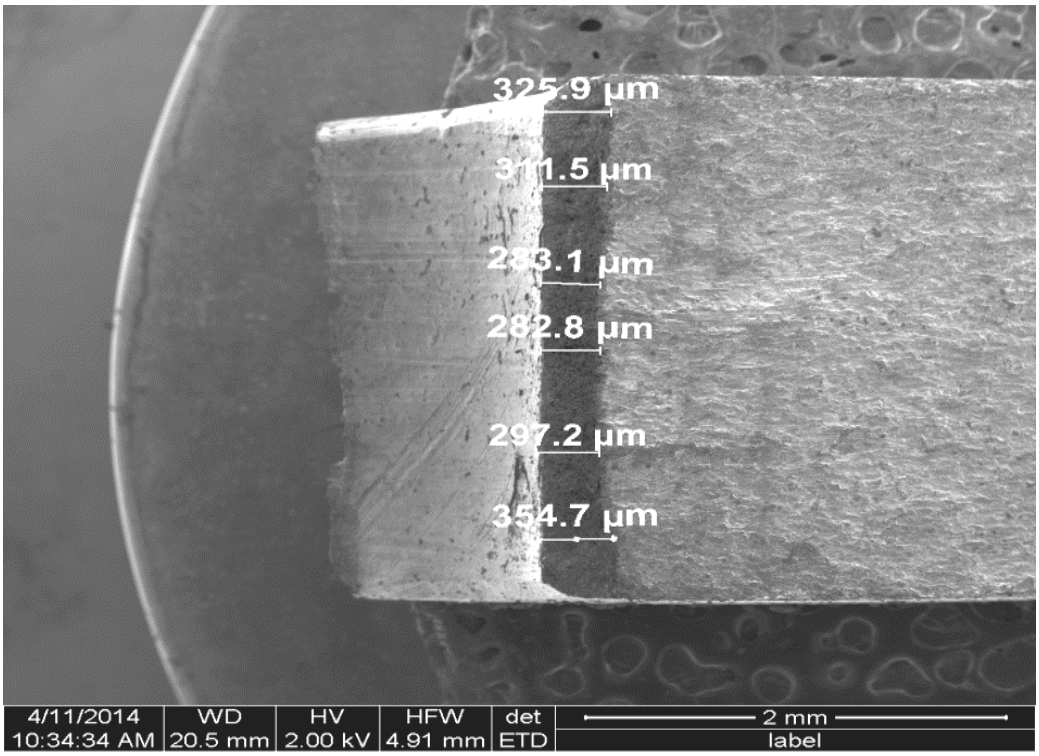

Figure 4.6: SEM through measurements made at different locations along the 2Al-03 specimen, thickness used for an average pit size calculation.

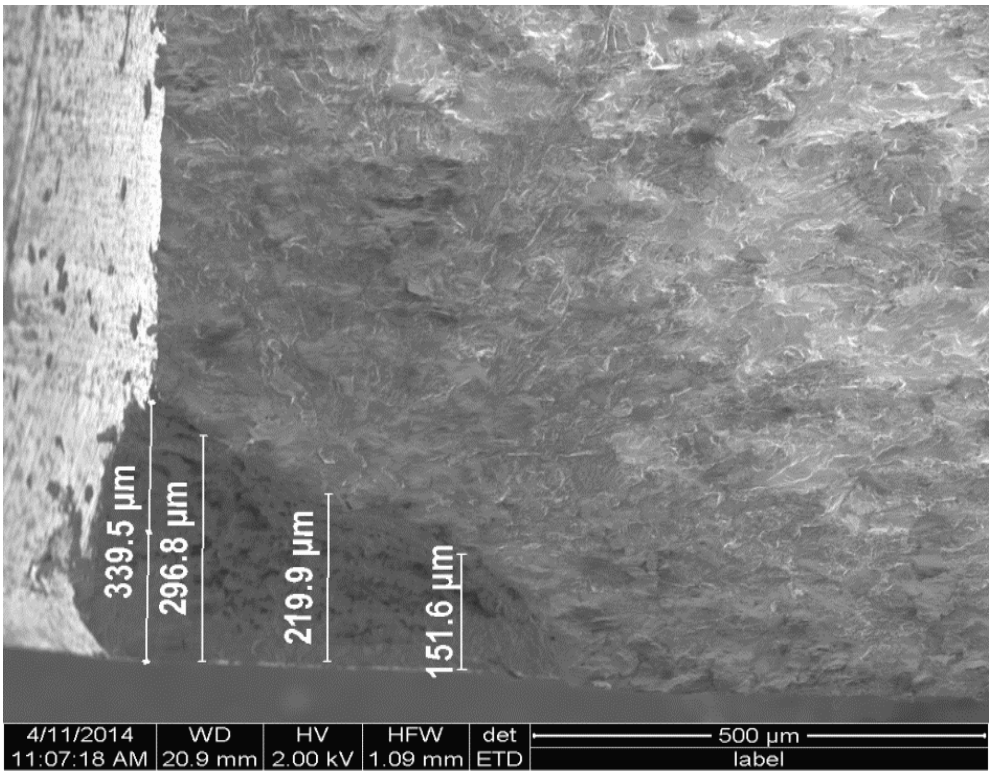

Figure 4.7: SEM measurements of the pit for specimen 2AS-03.

Using the SEM, the crack initiation at the corrosion pit could be detected with more detail compared to an optical microscope. For through pit specimens, the crack initiation occurred in a uniform manner regardless of the existence of multiple initiation locations. Micro-cracks typically started at several different areas. The micro-cracks grew briefly and after many cycles, these micro-cracks combined into a single crack front that continued to move through the specimen until reaching the boundary of the specimen. The SEM allows important finding in the crack initiation for the specimens with corner pit. Due to the geometry of the corner pit, there are fewer possible crack initiation locations than a through pit specimen. As a result, the crack initiation location can be narrowed down to a smaller, better defined region.

4.5 Discussion of Results

There is an inverse relationship between the stress intensity factor and the cycles until crack initiation based on experiments. When the stress intensity factor increases number of cycles to initiate a crack decreases. However, the specimens that are exposed to saltwater (3.5%) develop fatigue cracks in fewer cycles than the similar specimen only exposed to laboratory air. This is true for both through and corner pit specimens as shown in Figure 4.8. As we can see, the fatigue life of the through pit and corner pit specimens decreased in a corrosive environment (3.5% saltwater), compared with a laboratory environment. This reduction was 90% for the specimens with through pit and 75% for the specimens with corner pit. Moreover, the required number of cycles for crack initiation for corner pit specimens is lesser than the one for through pit specimens. The number of cycles decreases up to 94% in air, and up to 88% in saltwater environment.

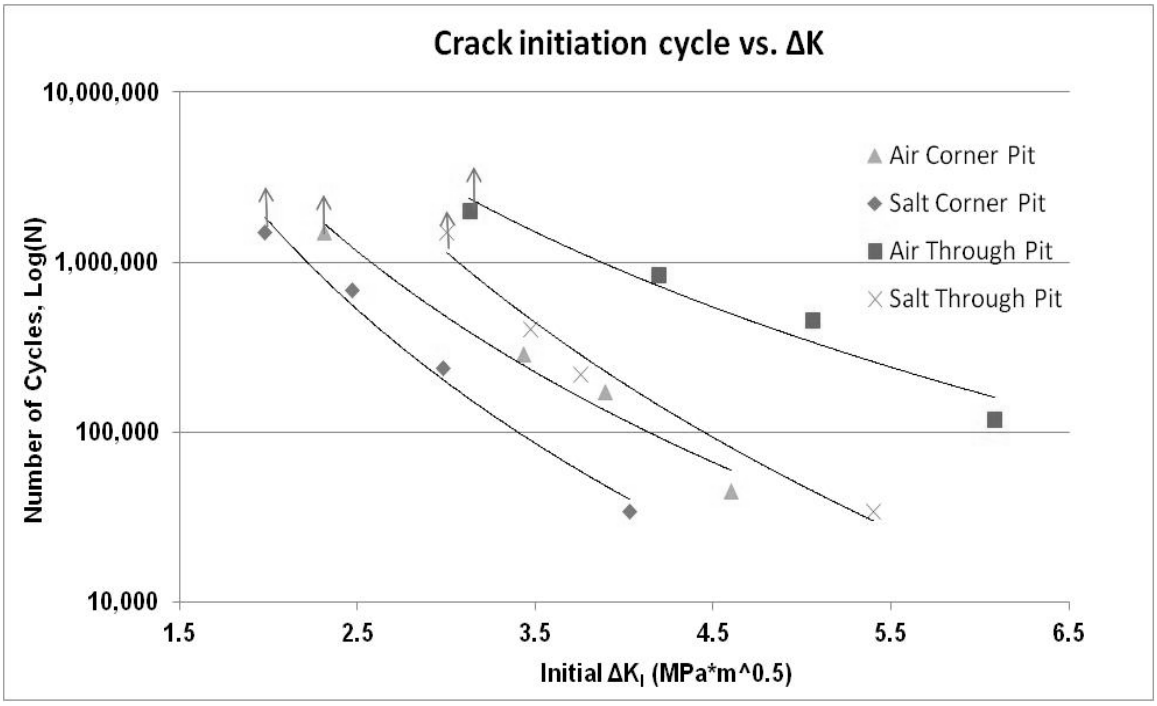

Figure 4.8: Number of cycles until crack initiation for all tested specimens vs. stress intensity range.

Correlating the crack growth rates of the current study with the previous ones conducted Misak et al. [25] was an important result as shown in Figure 4.2a. The crack growth rates versus stress intensity range for current research with chemically corroded through pit specimen and the previous ones with machined notch specimens showed no noticeable difference between two types of imperfections. The figure shows a higher growth rate for the saltwater exposed specimens than the laboratory air exposed specimens. The aggressive environment increases crack growth rate approximately 65% at a given stress intensity factor range.

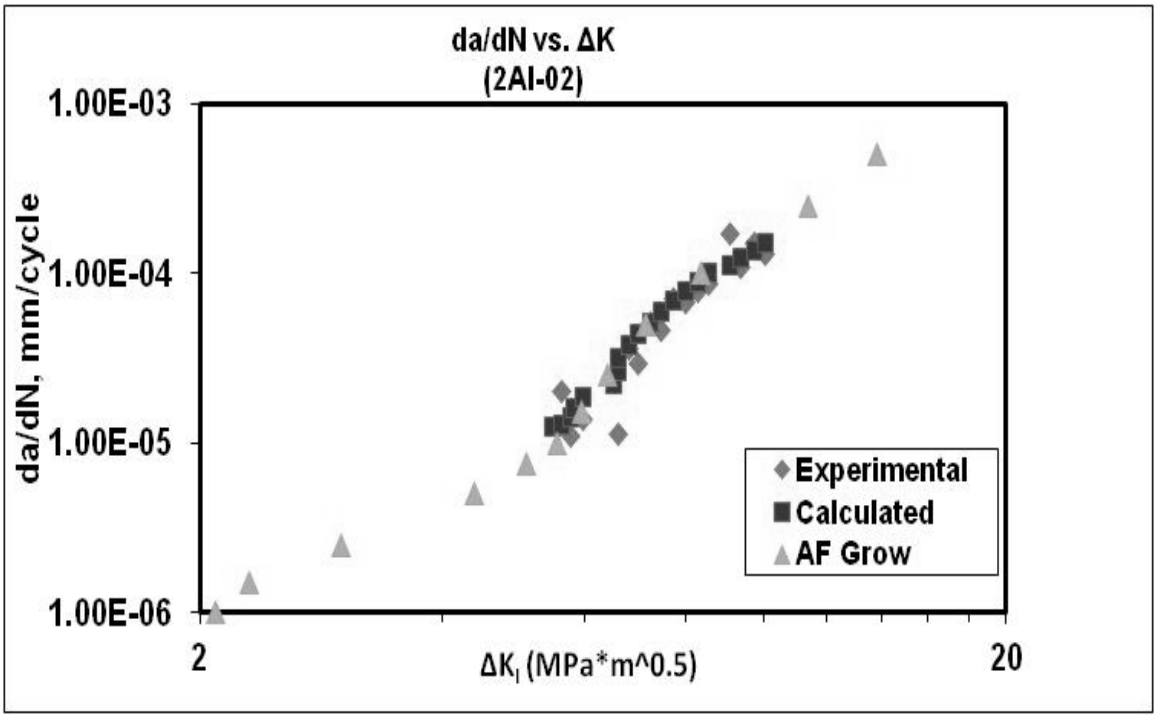

Figure 4.9: The crack growth rate of the through pit specimen 2AI-02 as a function of the stress intensity factor range. There is little variation between the current and AFGROW result [1].

On the other hand, Figure 4.9 shows experimental and measurement crack growth rate versus stress intensity range, in which the experimental data matches with the standard AFGROW data. It is a commonly used program that was developed by Air Force for predicting of crack growth of materials. This program has experimental database on fatigue crack growth for different materials and different stress ratios.

Additionally, when we compare the results of the experiments done by Hunt [14] on 7075-T6 with the current experiments on 2024-T3 with the same conditions, number of cycles for crack initiation is less in the previous study for both types of corrosion pit as shown in Figures 4.10 and 4.11.

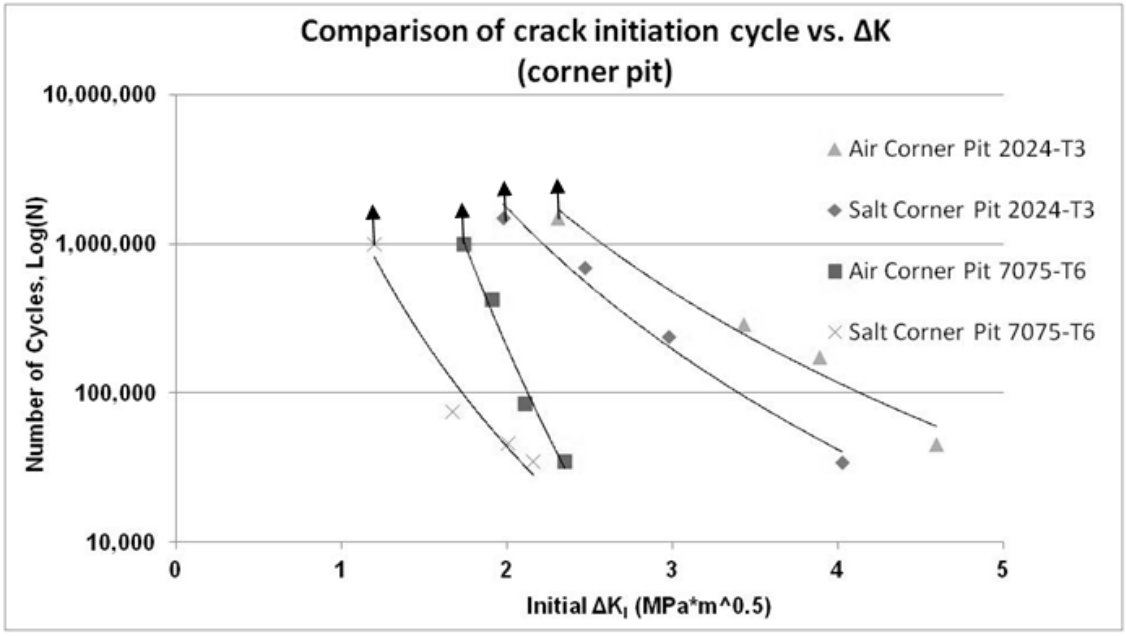

Figure 4.10: Number of cycles to crack initiation in 2024-T3 and 7075-T6 aluminum alloy for corner pit.

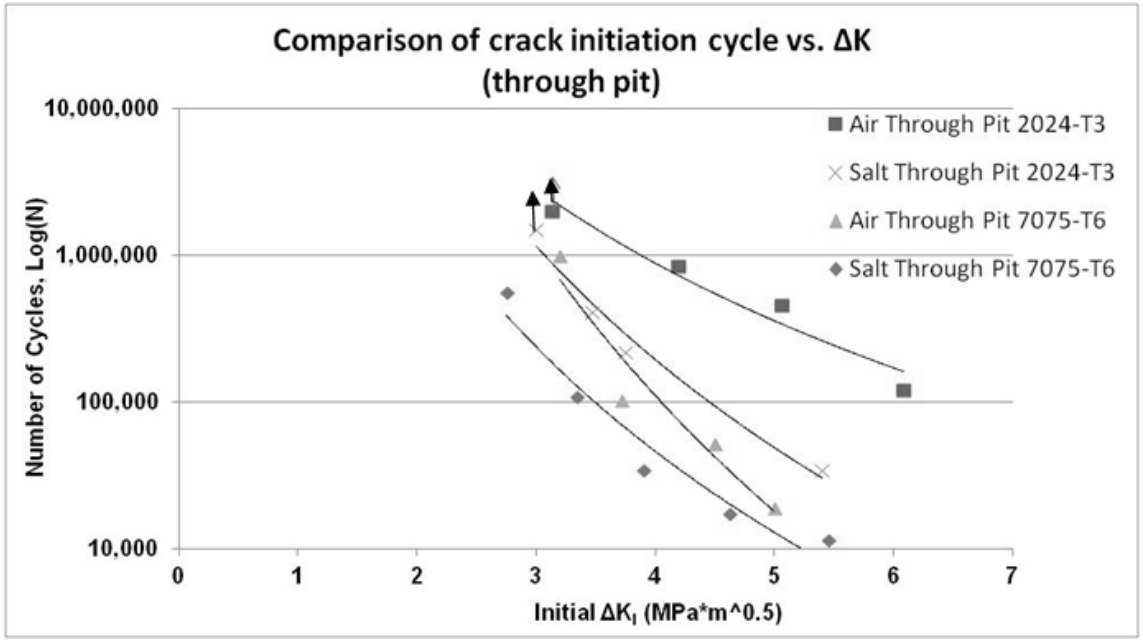

Figure 4.11 Number of cycles to crack initiation in 2024-T3 and 7075-T6 aluminum alloy for through pit.

For the corner pit, since the crack front is initially a quarter circle, it requires a certain number of cycles to grow into a full width through crack. Consequently, the crack growth rate may be firstly slower than the through pit specimens. Due to the difference in the stress state along the corrosion pit direction and through the thickness, the crack growth rate is different. During the corner crack growth, the growth of the crack behavior from the pit to a full width crack front shown in Figure 4.12.

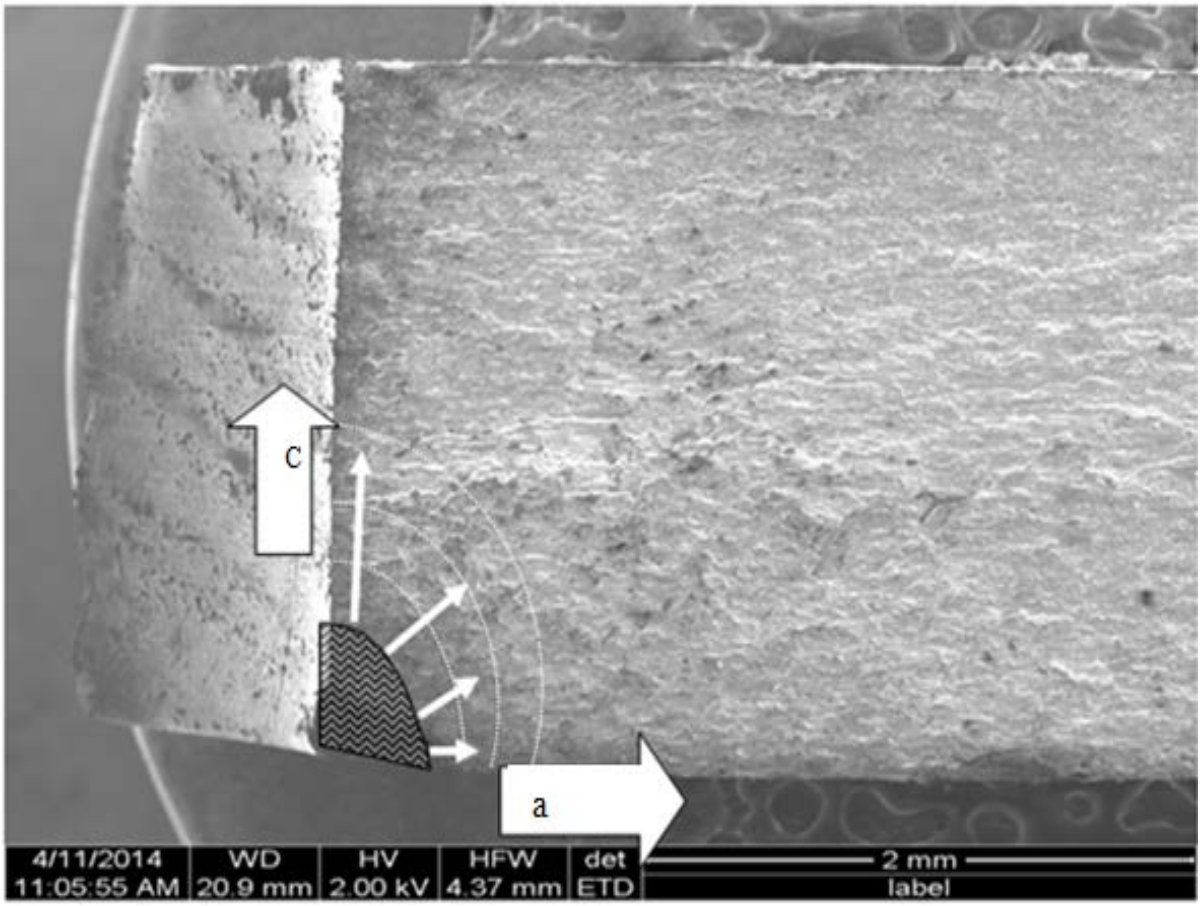

Figure 4.12: SEM photograph showing the change in aspect ratio, a/c, during the corner crack growth.

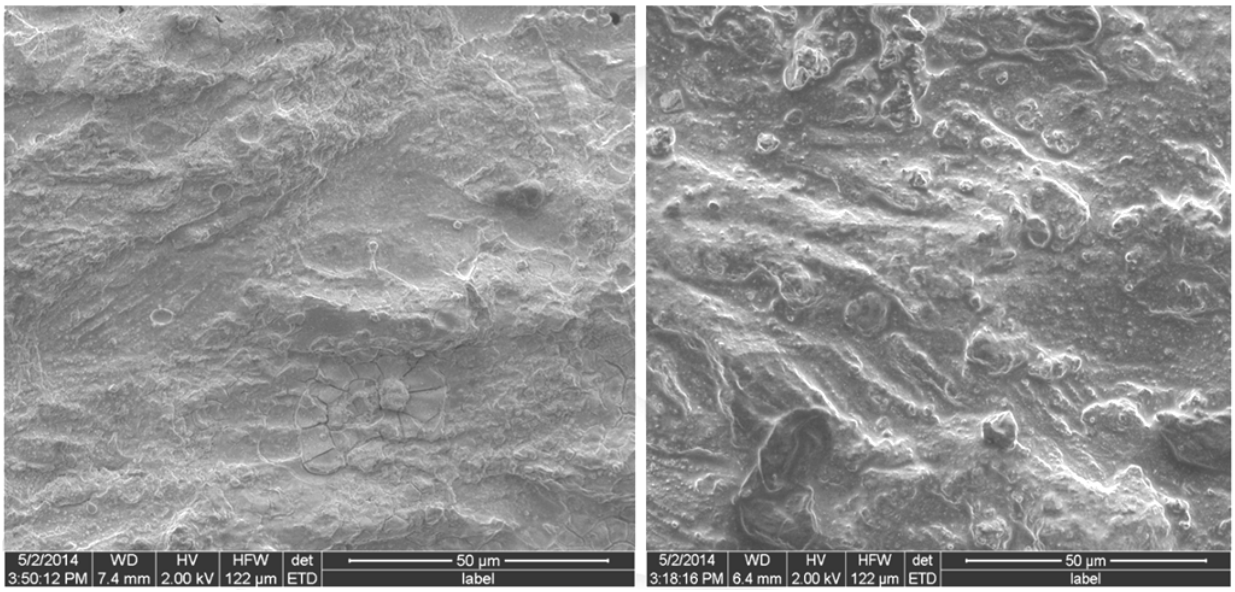

Figure 4.13a: SEM photograph showing fracture surface of saltwater environment for through pit (left) and corner pit (right).

Figure 4.13a shows fracture surface for through pit and corner pit in a saltwater environment. The left image shows the fracture surface for a through pit of uniaxial loading condition in salt environment, crack was along the plane of maximum mode I. The fracture surface was smooth, which is typical of planar slip dislocation mechanism. The right image shows a wavy surface for a saltwater corner pit in uniaxial loading condition. SEM images showing fracture surface of air environment for through pits and corner pits are shown in figure 4.13b. In the figure images 1, and 4 represent the fracture surfaces close to the corrosion pits. Because of planar slip dislocation mechanism these images exhibit a smooth region along the crack front. Images 2, and 5 show fracture surfaces of the region 0.25 mm away from corrosion pit these microstructure appears rough. Images 3, and 6 represent the surfaces 0.5 mm away from corrosion pit, in which microstructure looks more rough due to wavy slip dislocation mechanism.

Corner Pit **Through Pit**

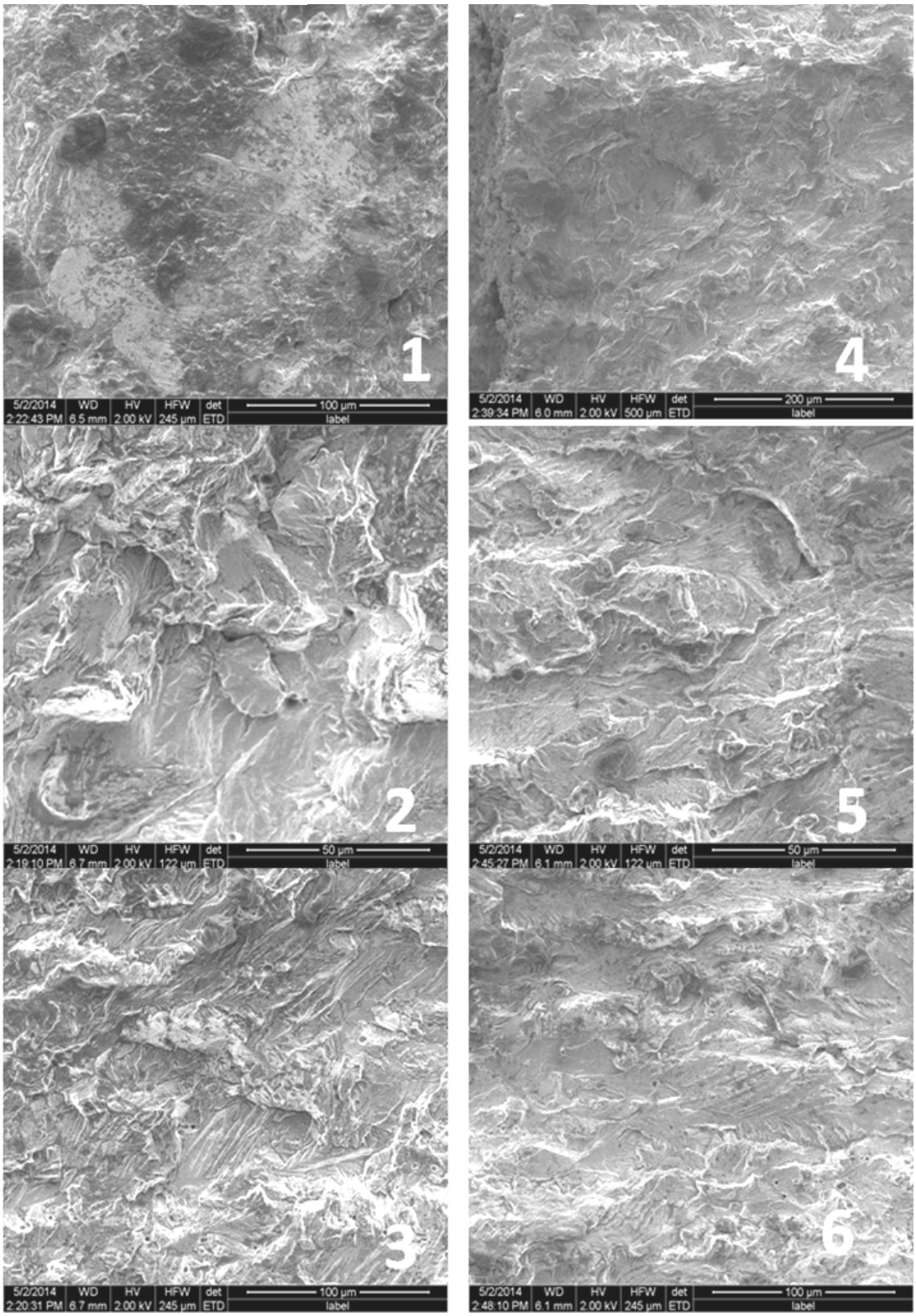

Figure 4.13b: SEM photograph showing fracture surface of air environment for through pit and corner pit.

5. Conclusions and Recommendations

5.1 Conclusions

The research conducted in this thesis investigated fatigue crack initiation and growth in 2024-T3 aluminum alloy specimens at through and corner pits in a central hole exposed to laboratory air and saltwater environments. Using the uni-axial MTS load frame, the specimens were cyclical loaded until crack length grew 17 mm. The experimental results captured the number of cycles until crack initiation as well as fatigue crack growth rate. In addition to the fatigue testing, the fracture surfaces were analyzed to examine the mechanisms of crack initiation for the fatigued specimens using SEM. Finite element analyses were used to calculate the stress intensity factor. The following conclusion could be made.

- In a corrosive environment, the required number of cycles for crack initiation decreases for both types of corrosion pits relative to those in laboratory environment. The number of cycles decreases up to 90% for through pits, and up to 75% for corner pits.
- In a corrosive environment, the crack growth is faster than laboratory air environment at a given ΔK.
- The required number of cycles for crack initiation for corner pit specimens is less than the one for through pit specimens. The number of cycles decreases up to 94% in air, and up to 88% in saltwater environment.
- Corner pit specimens have a slower crack growth rate than through pit specimens.

- Closed form solution is not accurate in calculating stress intensity range for the specimen with corner pit until the crack reaches the other side of the surface. Finite element model is needed to calculate stress intensity factor range for corner pit.
- In 2024-T3, the shape and size of pit are major factors affecting fatigue crack nucleation.
- There is a good agreement between crack growth rates for the specimen with machined notch and the specimen with through pit.

5.2 Recommendations

Due to the variability that is natural with materials testing, further testing on the fatigue crack growth from corrosion pits in 2024-T3 Al should be conducted. To simulate real life boundary conditions, further test parameters need to be considered such as:

- Different shape and depth of corrosion pit
- Multiple pits

Also, more FE modeling effort needs to be included for future research to include complicated geometries and test conditions

Appendix A: Finite Element Details

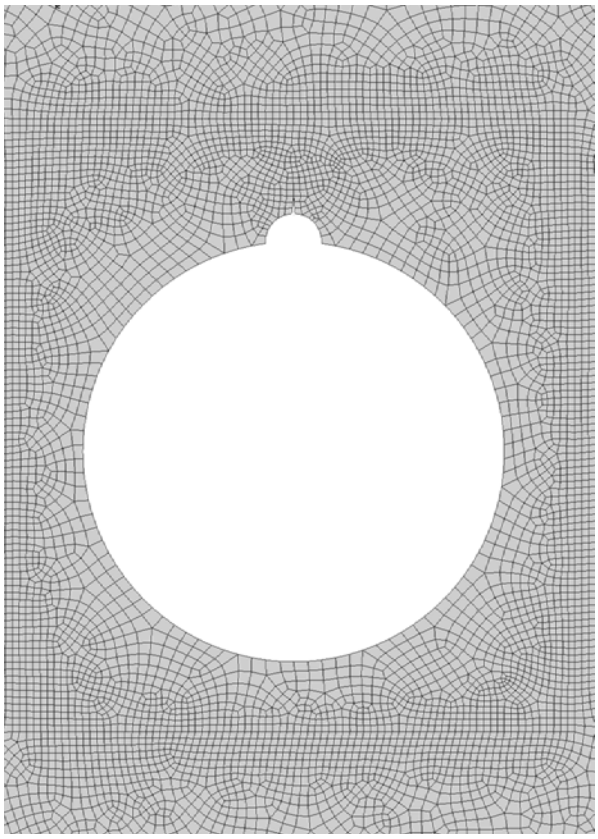

Figure A.1: Mesh of a uni-axial specimen with the crack length of 0.25 mm around the crack tip.

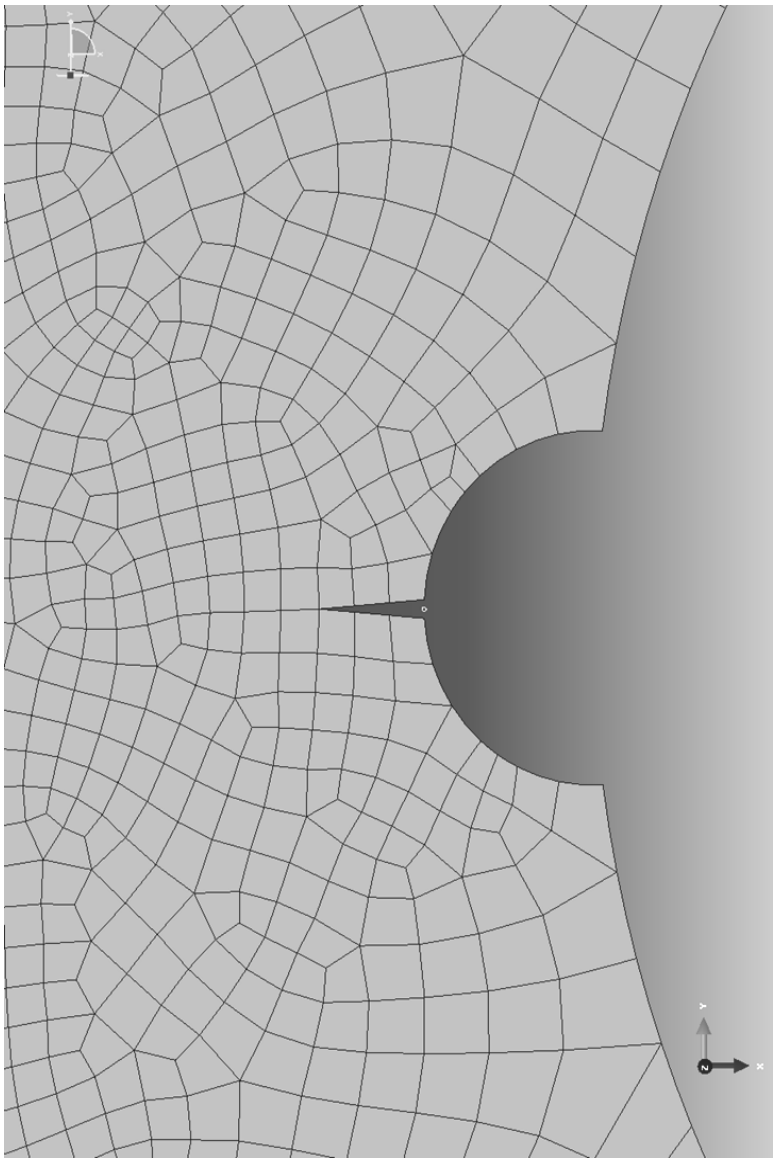

Figure A.2: Finite element model with crack length of 0.25 mm

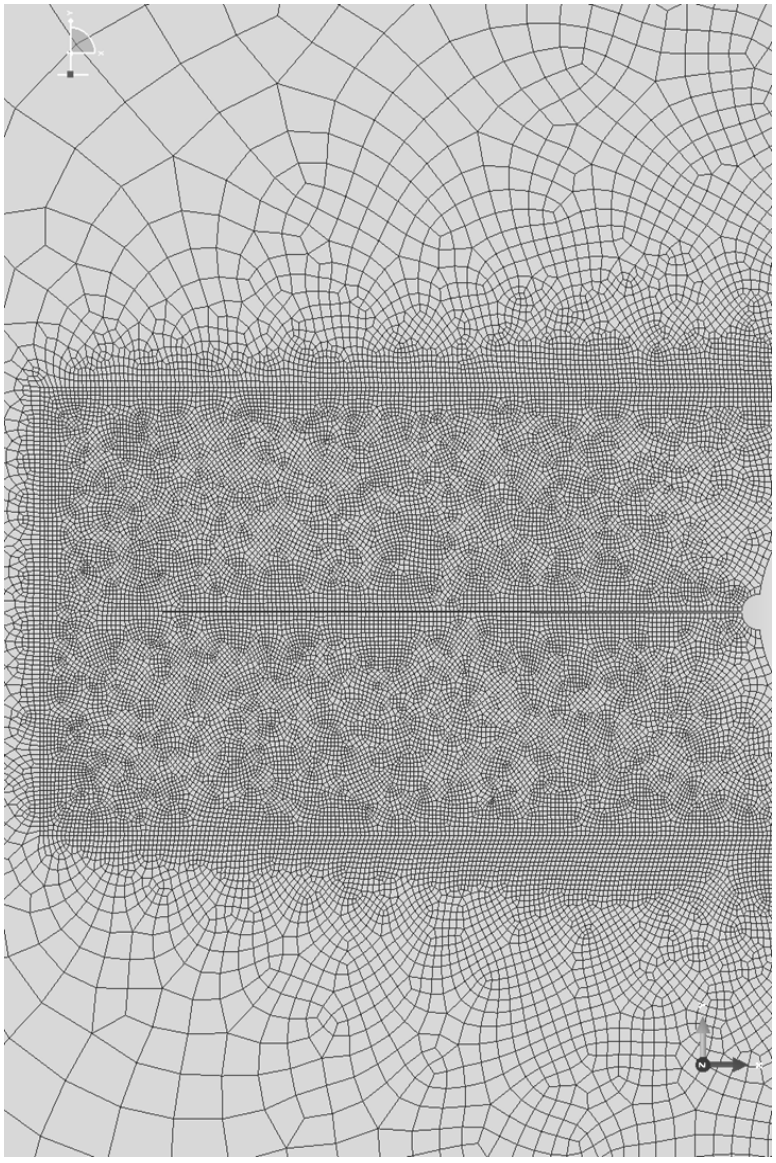

Figure A.3: Finite element model with crack length of 15 mm.

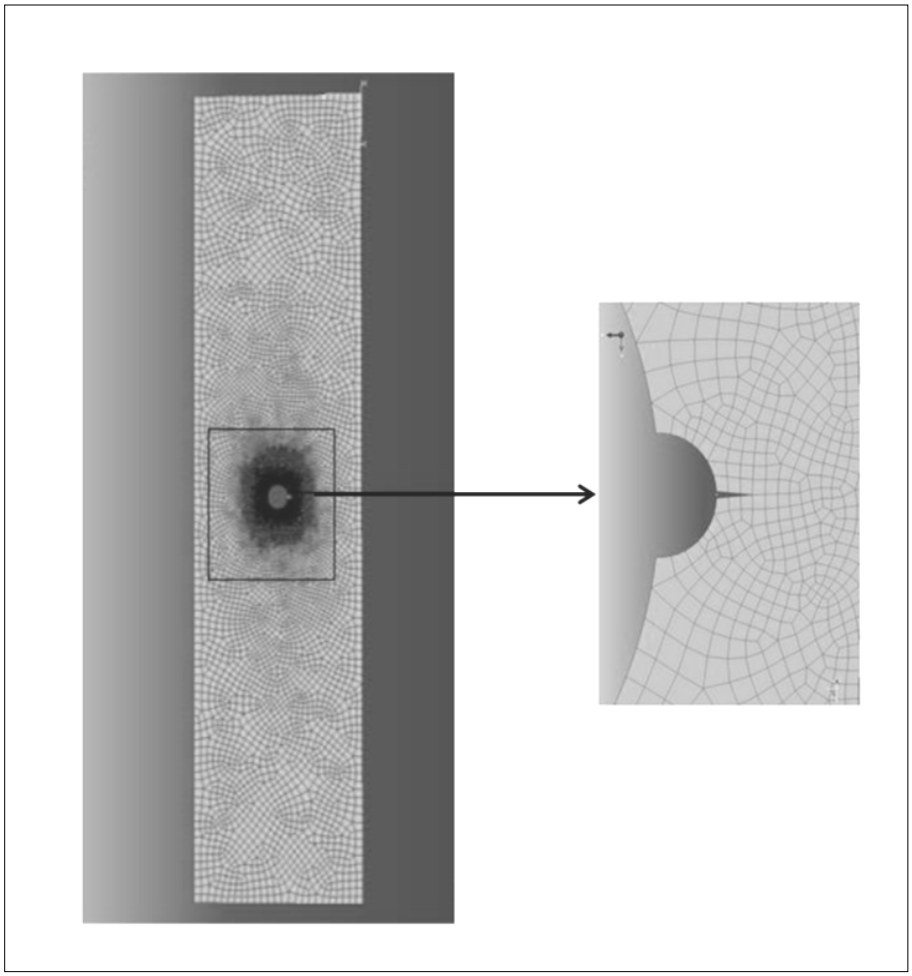

Figure A.4: Mesh created by Abaqus for the uni-axial specimen with a crack on a hole with refined mesh near the crack tip.

Appendix B: Crack Growth Plots for Through Pit Specimens

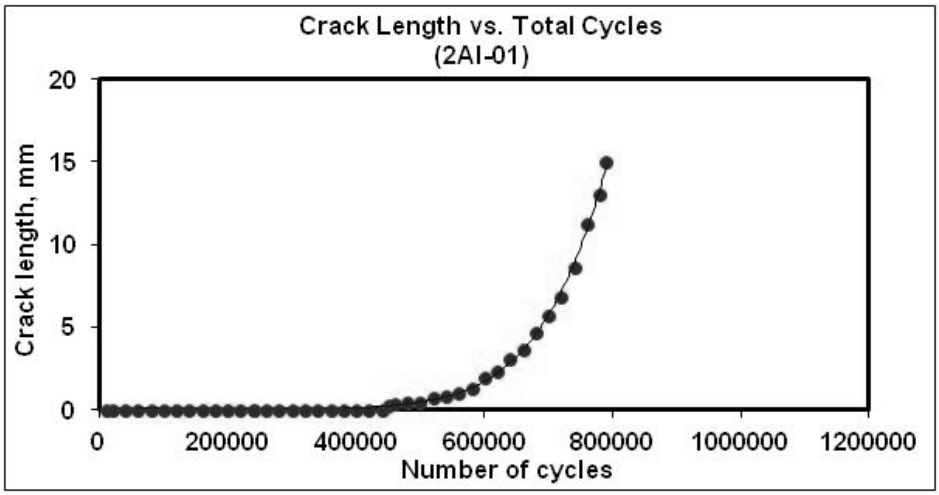

Figure B.1: The crack length vs. number of cycles during fatigue testing for the 2AI-01 specimen.

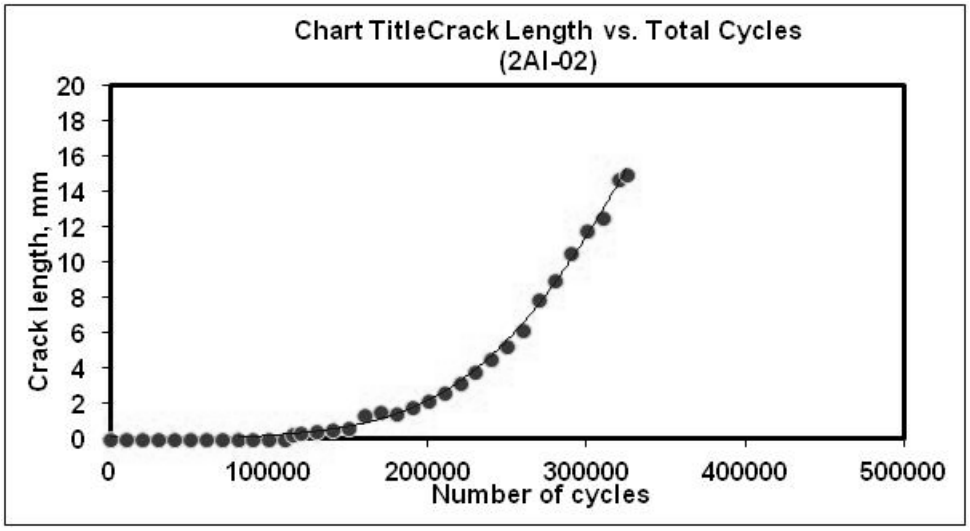

Figure B.2: The crack length vs. number of cycles during fatigue testing for the the 2AI-02 specimen.

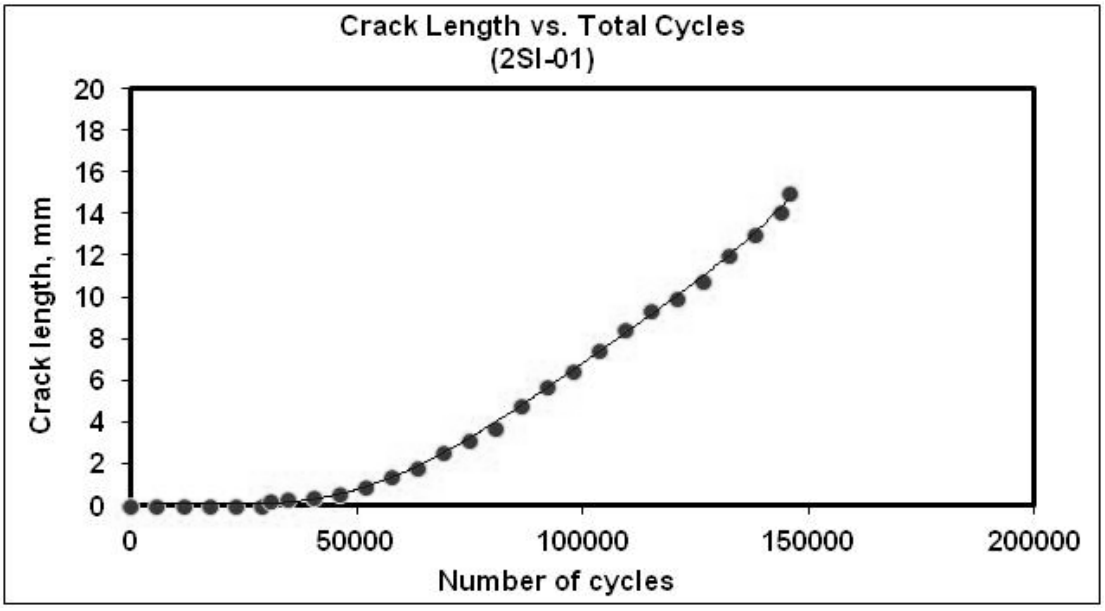

Figure B.3: The crack length vs. number of cycles during fatigue testing for the 2Sl-01 specimen.

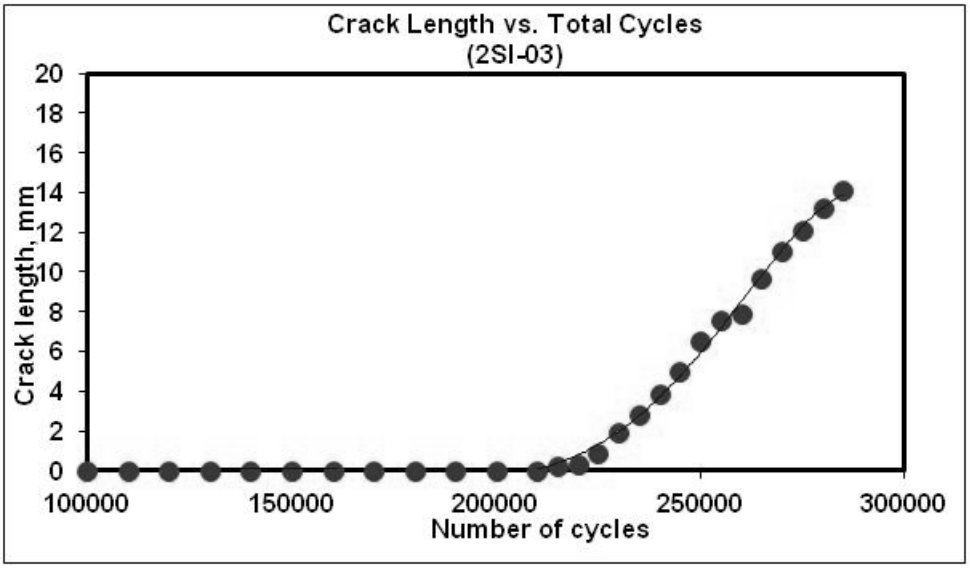

Figure B.4: The crack length vs. number of cycles during fatigue testing for the 2Sl-03 specimen.

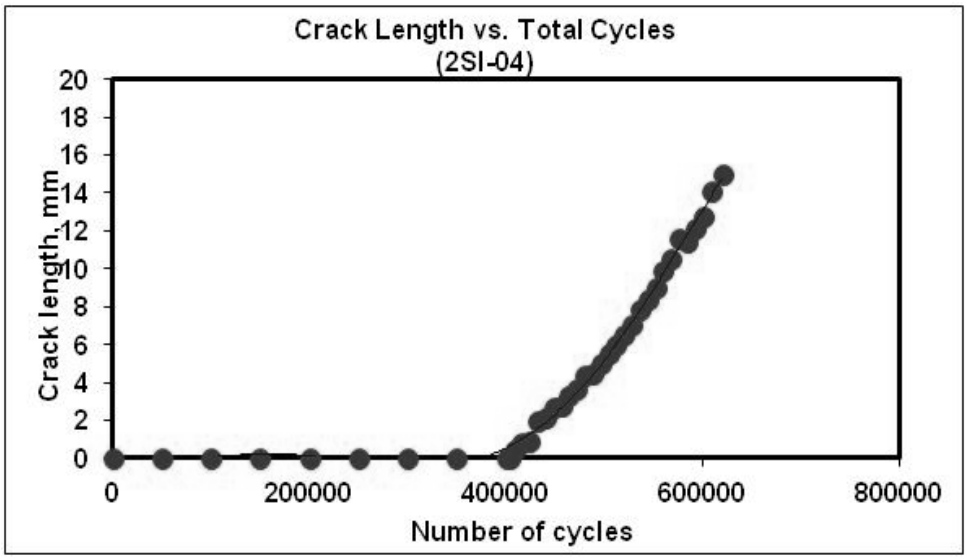

Figure B.5: The crack length vs. number of cycles during fatigue testing for the 2Sl-04 specimen.

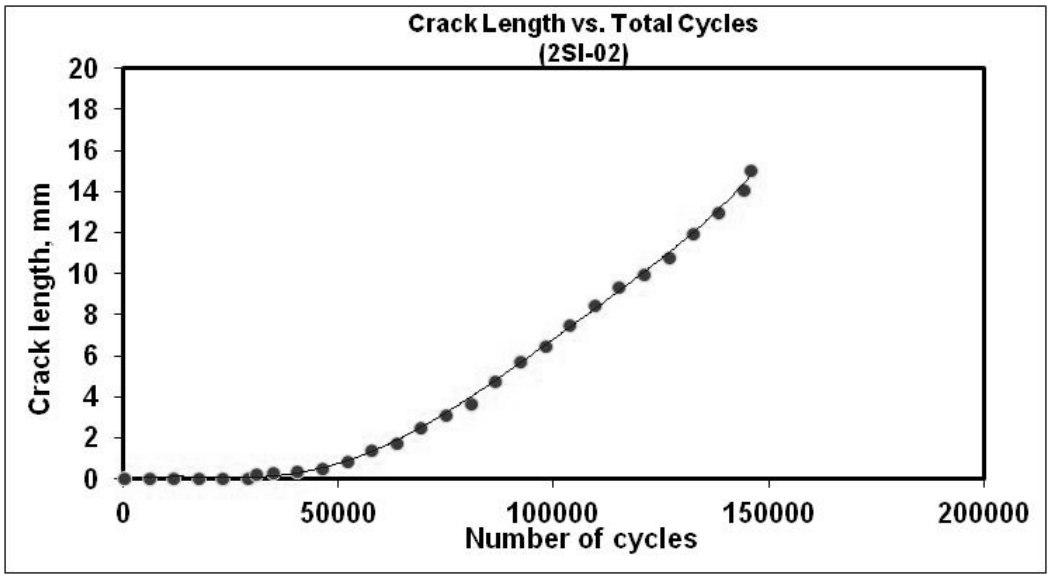

Figure B.6: The crack length vs. number of cycles during fatigue testing for the 2Sl-02 specimen that has no crack.

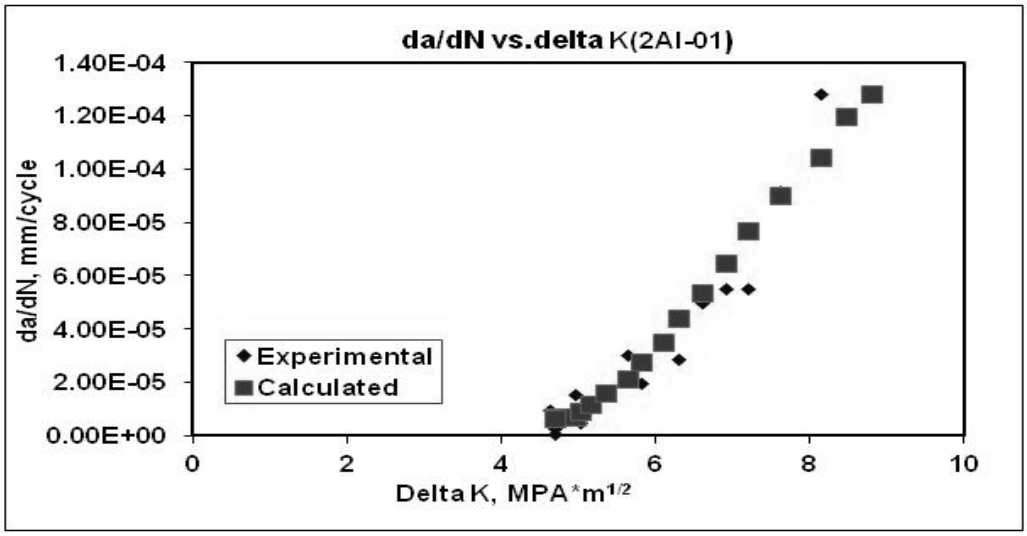

Figure B.7: Crack growth rate vs. the stress intensity range for 2Al-01 specimen.

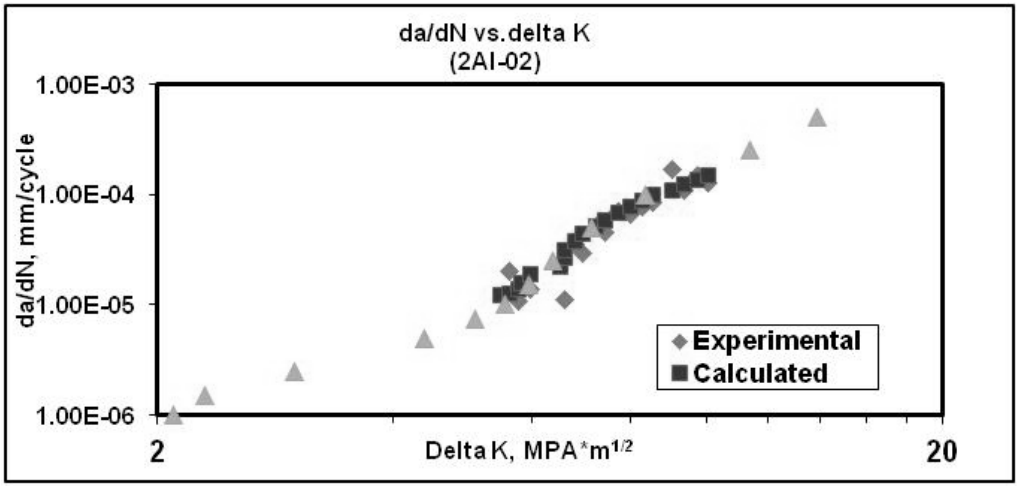

Figure B.8: Plot of crack growth rate vs. the stress intensity range for 2Al-02.

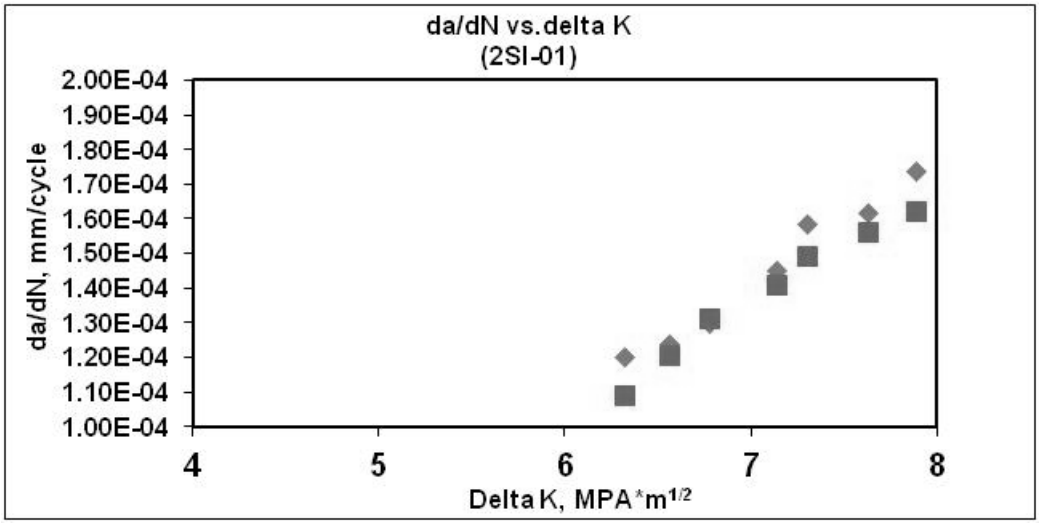

Figure B.9: Plot of crack growth rate vs. the stress intensity range for 2Sl-01.

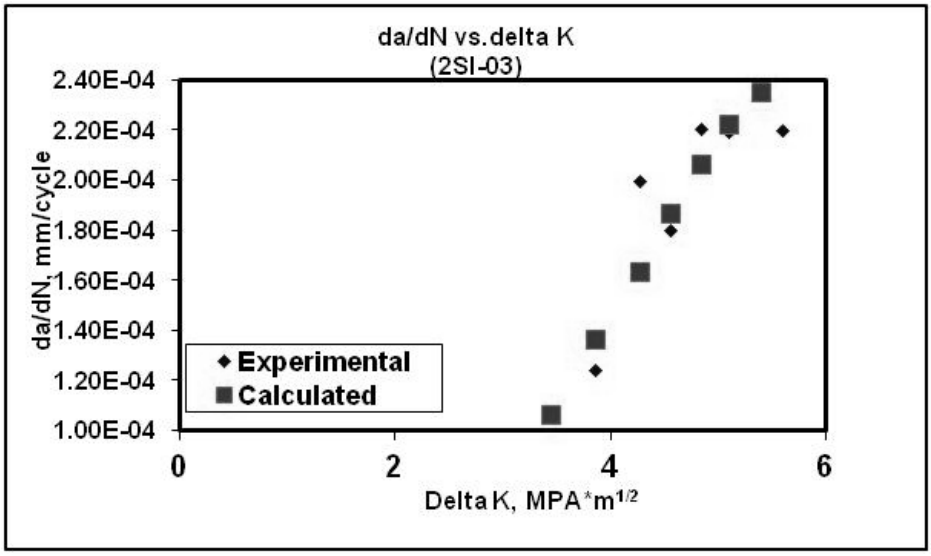

Figure B.10: Plot of crack growth rate vs. the stress intensity range for 2Sl-03.

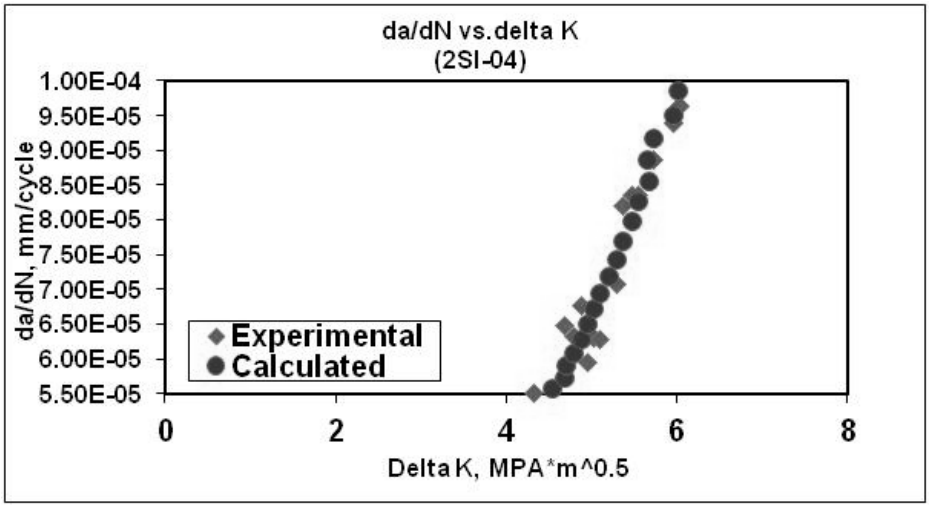

Figure B.11: Plot of crack growth rate vs. the stress intensity range for 2Sl-04.

Appendix C: Crack Growth Plots for Corner Pit Specimens

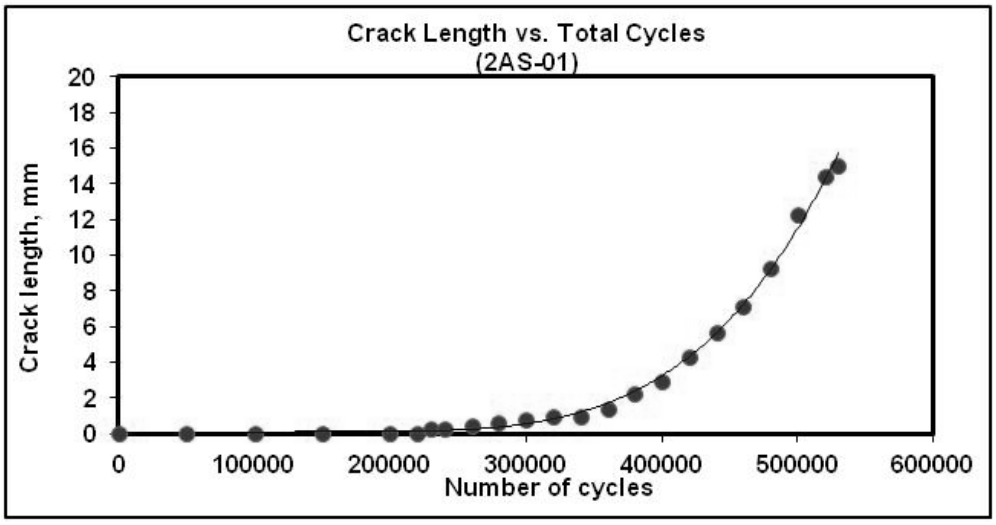

Figure C.1: The crack length vs. number of cycles during fatigue testing for the 2AS-01specimen.

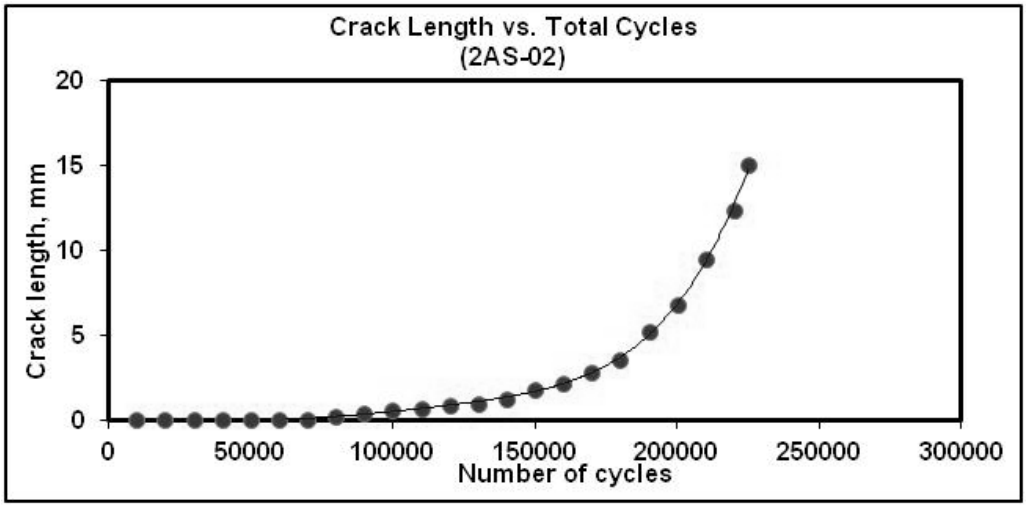

Figure C.2: The crack length vs. number of cycles during fatigue testing for the 2AS-02 specimen.

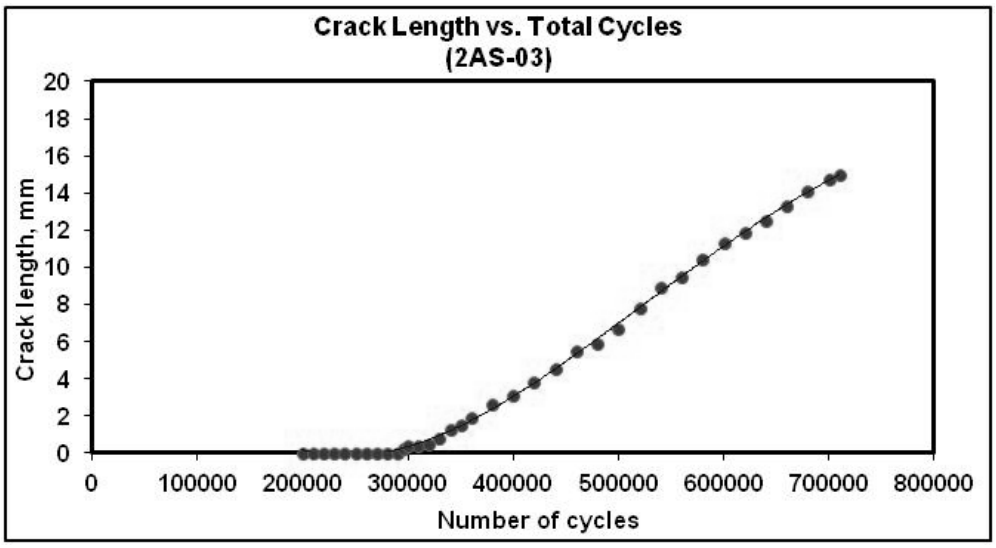

Figure C.3: The crack length vs. number of cycles during fatigue testing for the 2AS-03 specimen.

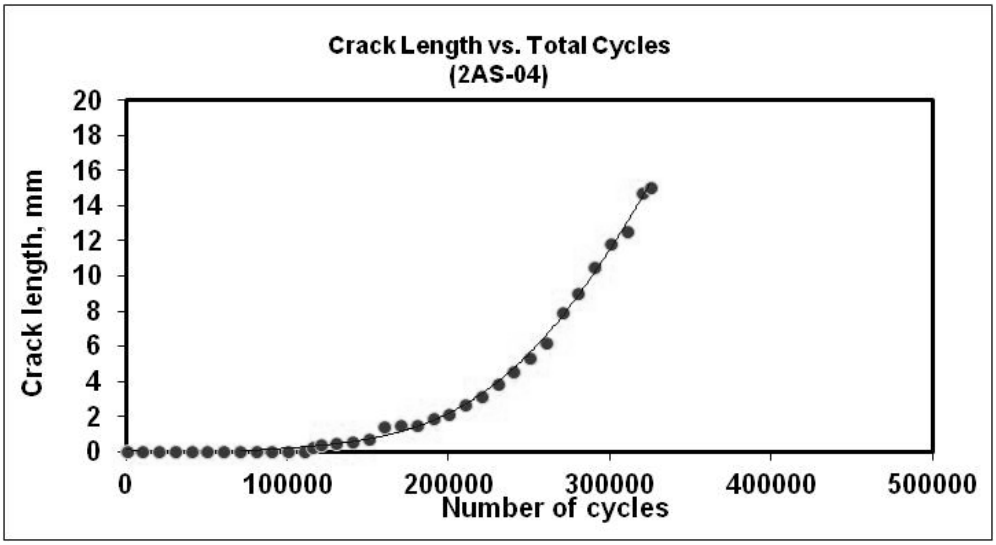

Figure C.4: The crack length vs. number of cycles during fatigue testing for the 2AS-04 specimen.

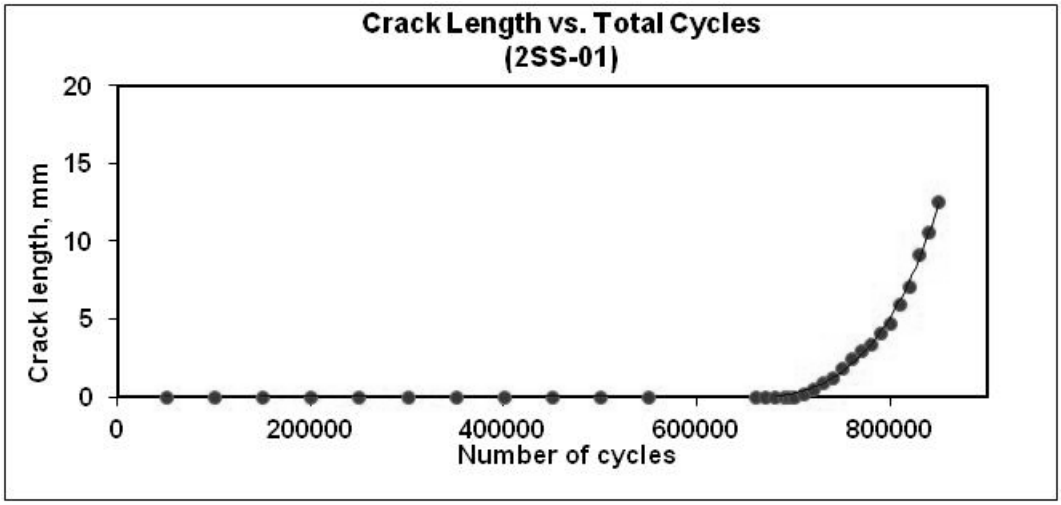

Figure C.5: The crack length vs. number of cycles during fatigue testing for the 2SS-01 specimen.

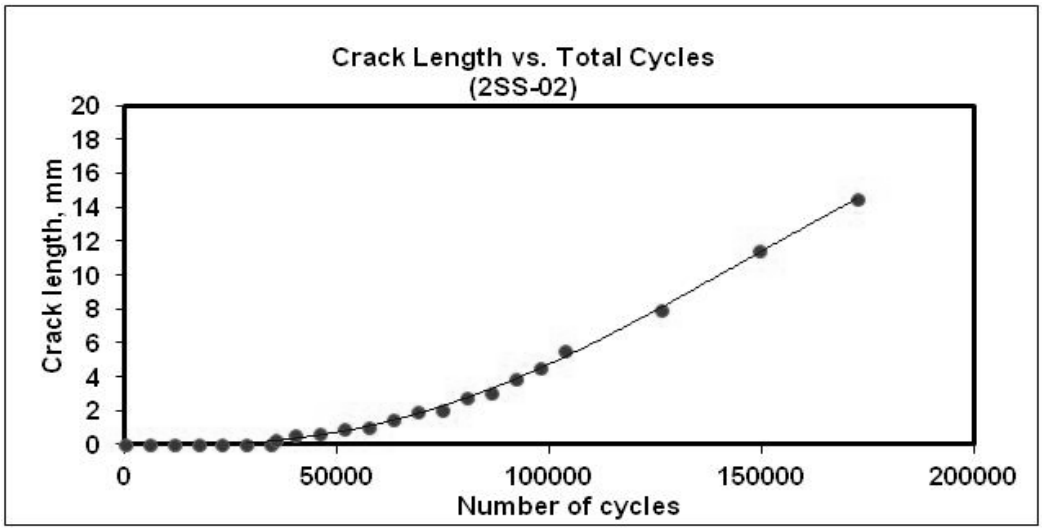

Figure C.6: The crack length vs. number of cycles during fatigue testing for the 2SS-02 specimen.

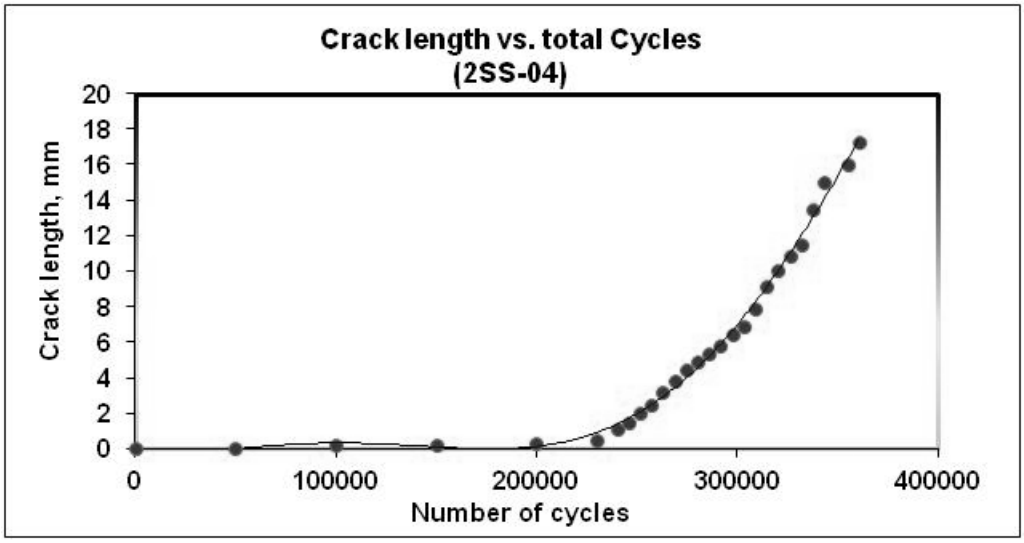

Figure C7: The crack length vs. number of cycles during fatigue testing for the 2SS-04 specimen.

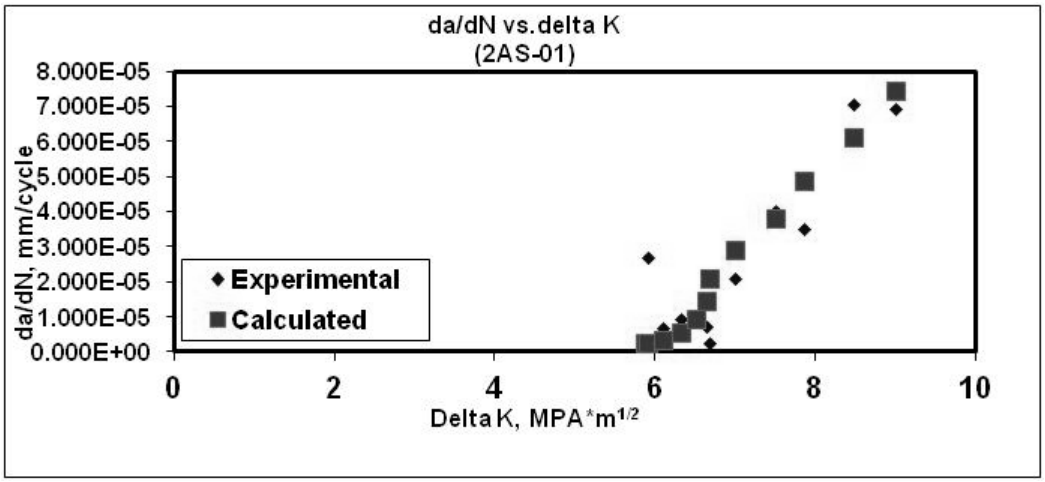

Figure C.8: Plot of crack growth rate vs. the stress intensity range for 2AS-01.

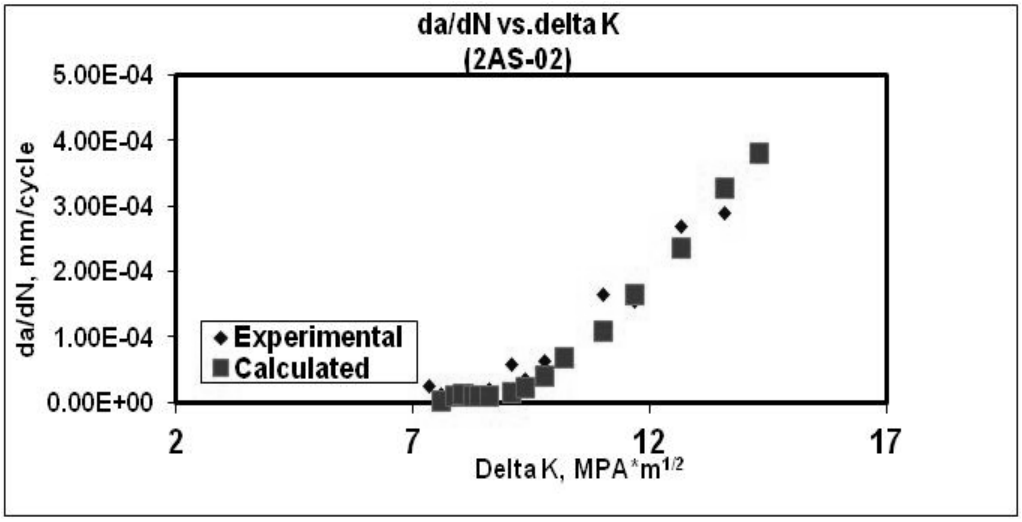

Figure C.9: Plot of crack growth rate vs. the stress intensity range for 2AS-02.

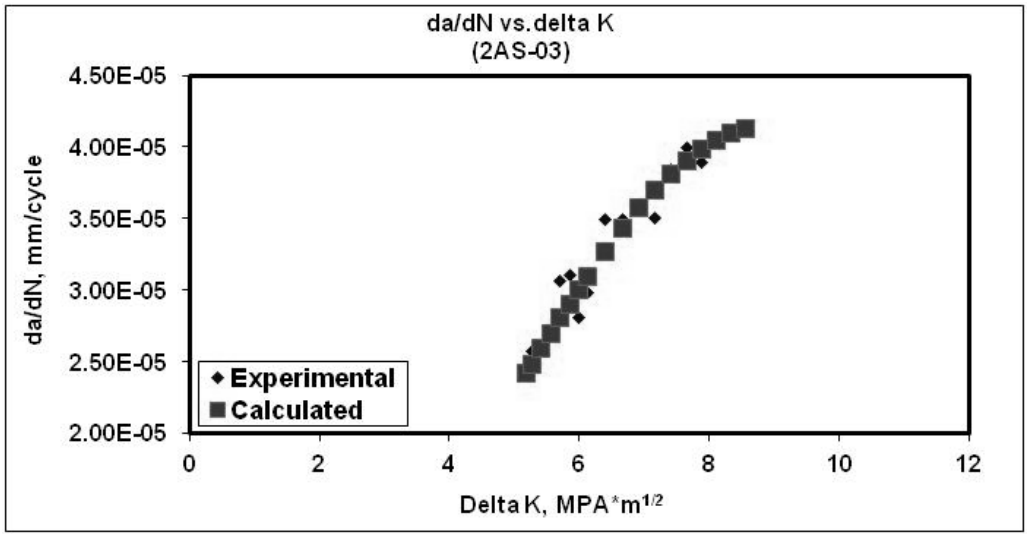

Figure C.10: Plot of crack growth rate vs. the stress intensity range for 2AS-03.

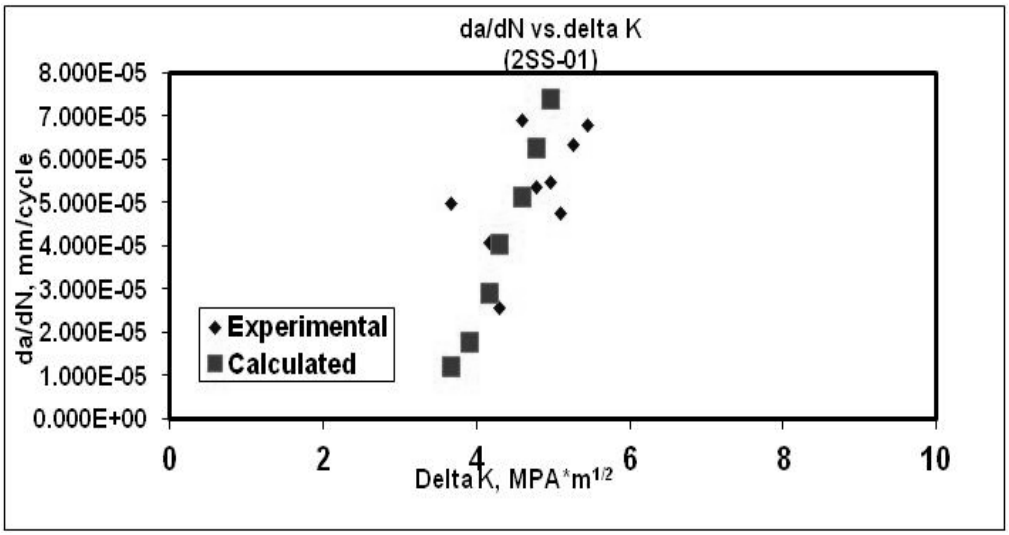

Figure C.11: Plot of crack growth rate vs. the stress intensity range for 2SS-01.

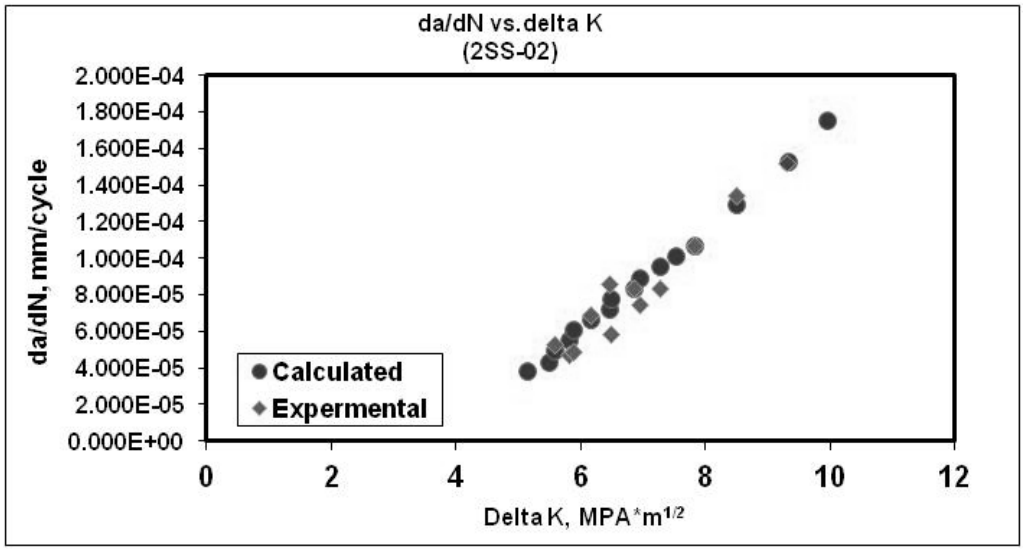

Figure C.12: Plot of crack growth rate vs. the stress intensity range for 2SS-02.

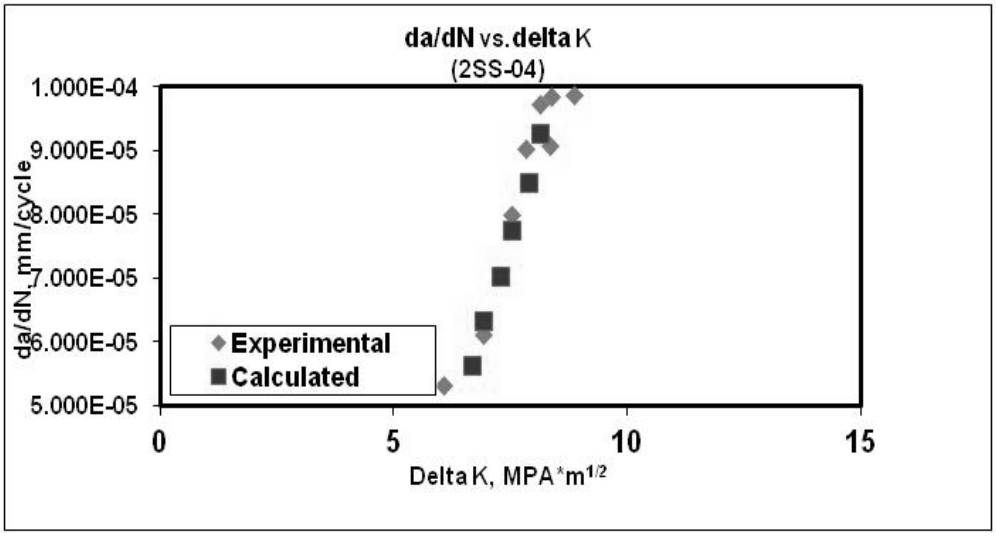

Figure C.13: Plot of crack growth rate vs. the stress intensity range for 2SS-04.

Appendix D: SEM Photographs

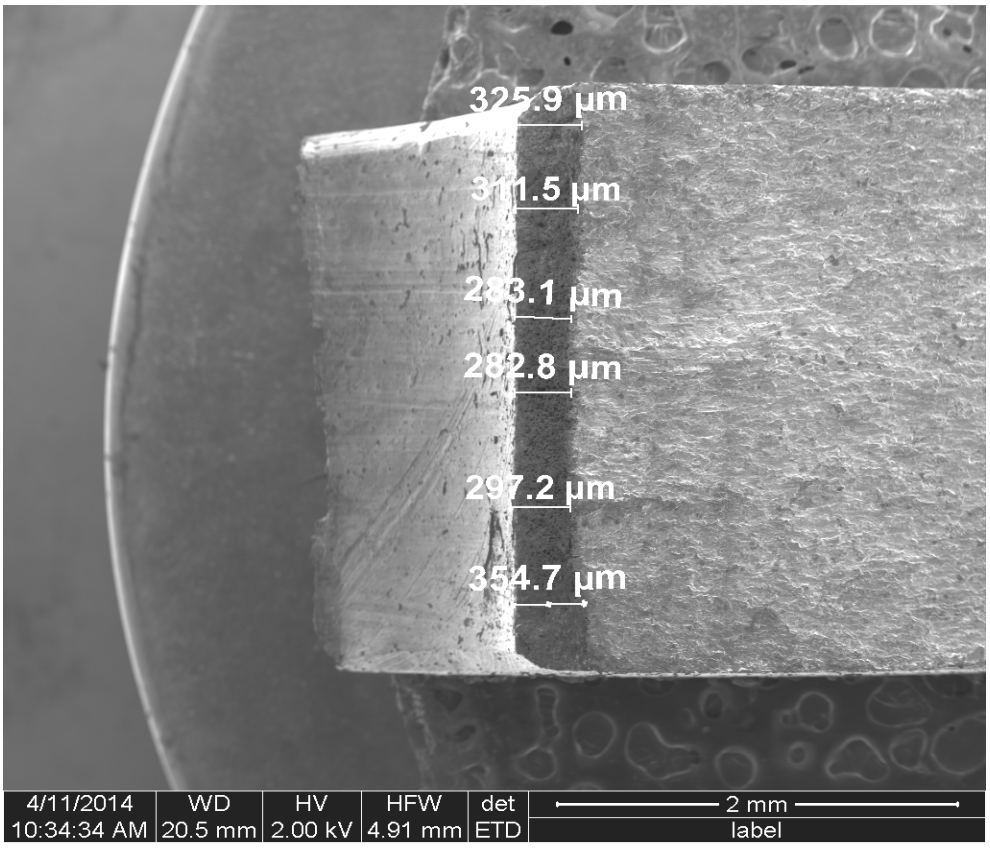

Figure D.1: Side view of the through pit specimen 2Al-03 using the SEM. Measurements of the pit were taken at several locations therefore an average pit size could be calculated.

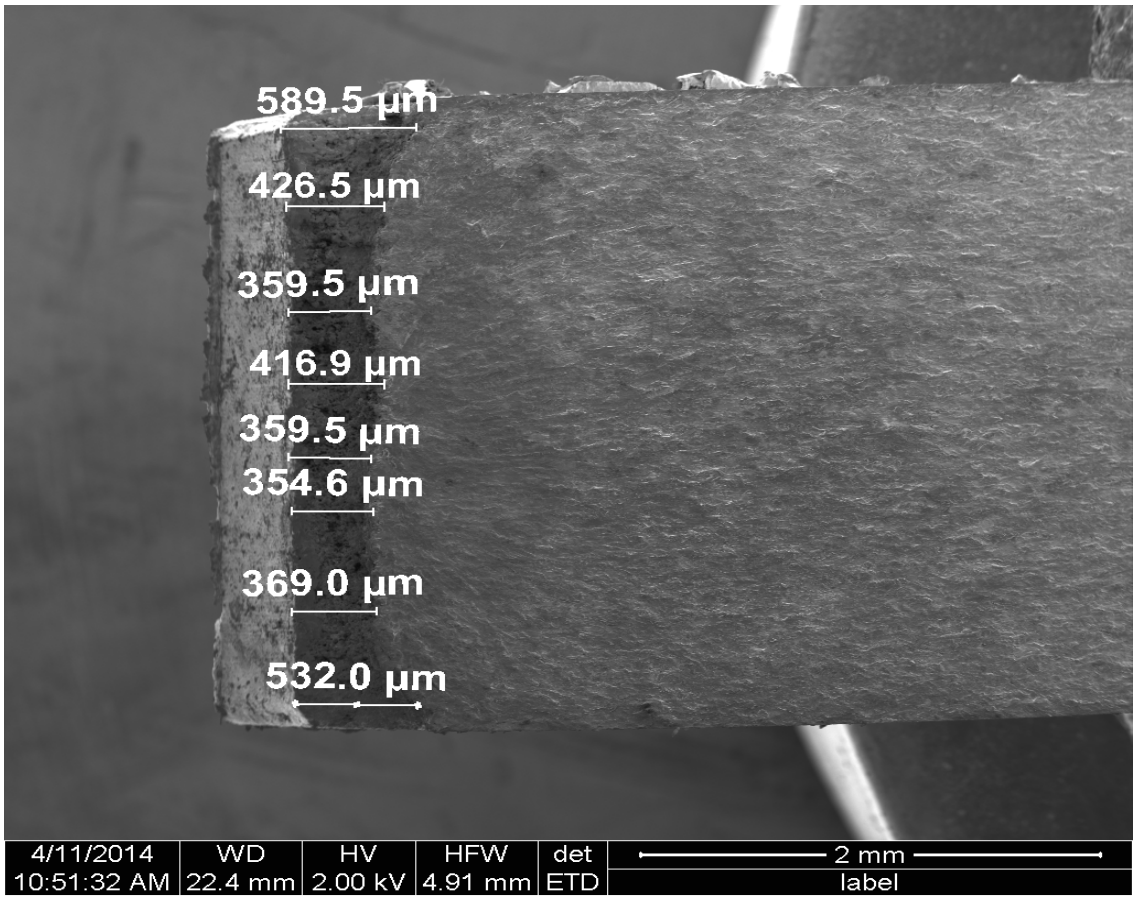

Figure D.2: Side view of the through pit specimen 2Sl-03 using the SEM. Measurements of the pit depth were taken at several locations therefore an average pit size could be measured.

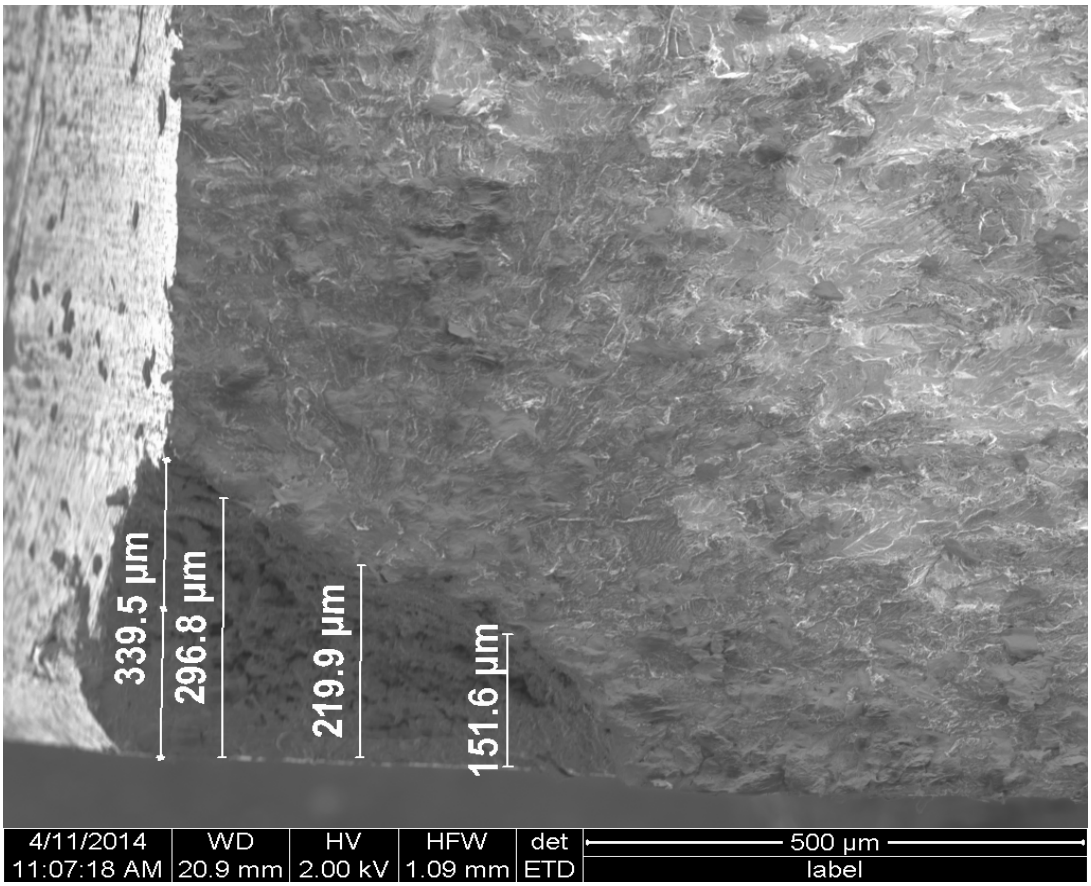

Figure D.3: Side view of the through pit specimen 2AS-03 using the SEM. Measurements of the pit size were taken at several locations therefore an average pit size could be calculated.

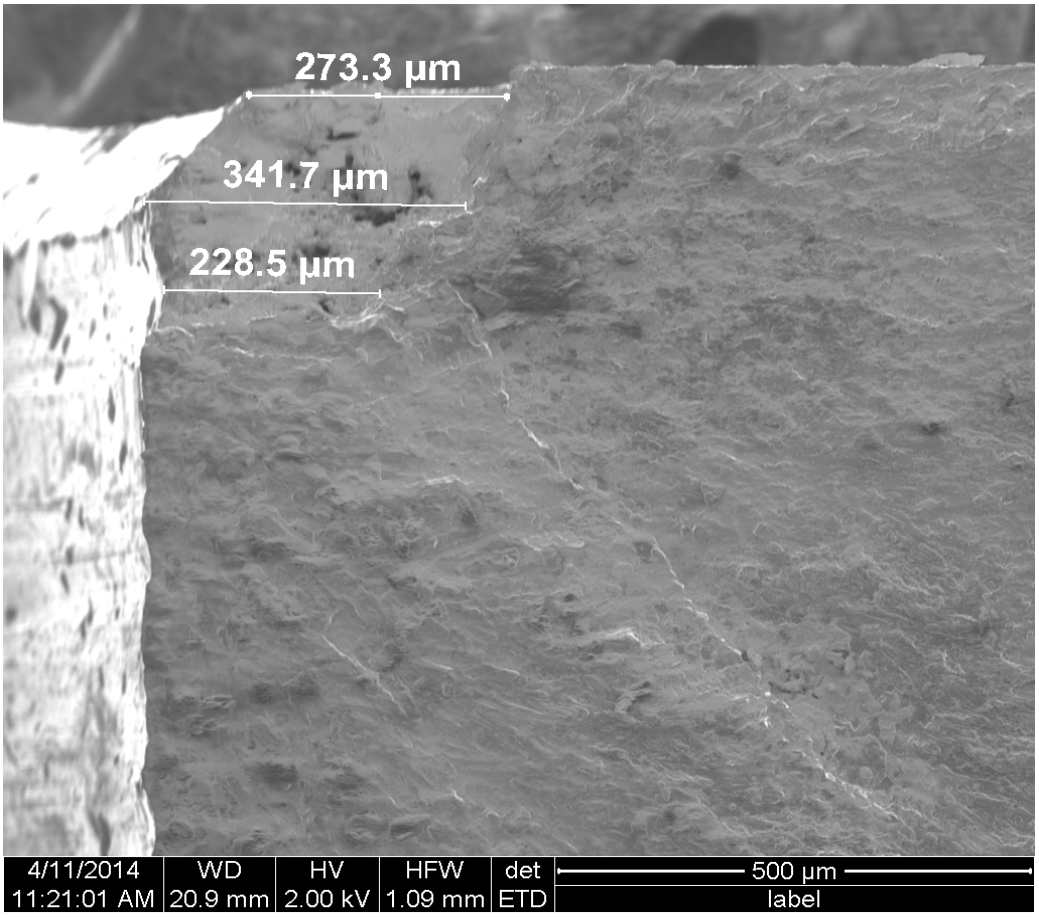

Figure D.4: Side view of the through pit specimen 2SS-02 using the SEM. Measurements of the pit size were taken at several locations therefore an average pit size could be calculated.

Bibliography

[1] AFGROW, 2013. Retrieved from http://www.afgrow.net/

[2] Anderson, T.L. Fracture Mechanics: Fundamentals and Applications. Taylor and Francis, 2005.

[3] Bolotin, V. V. Mechanics of Fatigue. Boca Raton: CRC, 1999.

[4] Burns, J.T., J.M. Larsen, and R.P. Gangloff. "Driving forces for localized corrosion-to-fatigue crack transition in AlZnMgCu". *Fatigue and Fracture of Engineering Materials and Structures*, 34(0):745 – 773, 2011. ISSN 1460-2695.

[5] Burns, J.B. "The effect of initiation feature and environment on fatigue crack formation and early propagation in Al-Zn-Mg-Cu." PhD Dissertation, University of Virginia, 2010.

[6] Chen, G.S., K.C.Wan, M. Gao, R.P.Wei, and T.H. Flournoy. "Transition from pitting to fatigue crack growth modeling of corrosion fatigue crack nucleation in a 2024-T3 Al alloy". *Materials Science and Engineering*: A, 219:126-132, ISSN 0921-5093. 1996

[7] Clark, G. "A review of Australian and New Zealand investigations on aeronautical fatigue during the period April 2005 to March 2007". Air Vehicles Division Defense Science and Technology Organization, 2007. ISSN DSTO-TN-0747.

[8] Dowling, N.E. Mechanical Behavior of Materials.3rd ed. Pearson, 2007.

[9] DuQuesnay, D.L., P.R. Underhill, and H.J. Britt. "Fatigue crack growth from corrosion damage in 7075-T6511 aluminum alloy under aircraft loading". Dept of Mechanical Engineering, Royal Military College of Canada, 1996.

[10] Evans, U.R. The Corrosion and Oxidation of Metals. Hodder Arnold, 1968.

[11] Forman, R.G. “Study of fatigue crack initiation from flaws using fracture mechanics theory” AFFDL, WPAFB, OH, 1968.

[12] Gangloff, R. P. “Environmental cracking- corrosion fatigue” *Corrosion Tests and Standards Manual ASM International*, Metals Park, OH, 2004.

[13] Gangloff, R.P. “Hydrogen assisted cracking of high strength alloys”, *Elsevier Science,* 6:31-101, 2003.

[14] Hunt, E.M. “Crack initiation and growth behavior at corrosion pit in 7075-T6 high strength aluminum alloy”. MS Thesis, AFIT, WPAFB, OH, 2013.

[15] Jones, K. and D.W. Hoeppner. "Prior corrosion and fatigue of 2024-T3 aluminum alloy". *Corrosion Science,* 48:3109–3122, 2006.

[16] Kachanov, M., B. Shafiro, and I. Tsukrov. Handbook of Elasticity Solutions. Kluwer Academic Publishers, 2003.

[17] Koch, G.H. and E.L. Hagerdorn. “Effect of pre-existing corrosion of fatigue cracking of Al alloys 2024-T3 and 7075-T6”. Air Force Research Laboratory, WPAFB, OH, 1995.

[18] Lados, D.A. and P.C. Paris. “Parameters and key trends affecting fatigue crack growth: A tribute to Professor Arthur J. McEvily’s contributions”. *Materials Science and Engineering*: A, 468-470(0):70 – 73, 2007. ISSN 0921-5093.

[19] Lee, B. “Influence of pre-existing corrosion pits on fatigue life in a 2024-T3 Al alloy”. MS Thesis, Lehigh University, 1999.

[20] Lee, Y. and S.G. Dorman. “Effect of chromate primer on corrosion fatigue in Al alloy 7075”. *Proscenia Engineering*, 10:1220–1225, 2011. ISSN 1877-7058.

[21] Lindley, T.C., P. Mcintyre, and P. J. Trant , “Fatigue crack initiation at corrosion pits” *Metals Technology* , 9: 135-142, 1982.

[22] Lukas, P. and L. Kunz. “Small cracks nucleation, growth and implication to fatigue life”. *International Journal of Fatigue*, 25(0):855–862, 2003. ISSN 0142-1123.

[23] Lynch, S.P. “Progression markings, striations, and crack-arrest markings on fracture surfaces”. *Materials Science and Engineering*: A, 468-470(0):74–80, 2007. ISSN 0921-5093.

[24] Marcus, P. Corrosion Mechanisms in Theory and Practice. CRC Press, 2011.

[25] Misak, H.E., V.Y. Perel, V. Sabelkin, and S. Mall. "Biaxial tension-tension fatigue crack growth behavior of 2024-T3 under ambient air and salt water environments". Engineering Fracture mechanics 118:83-79, 2014.

[26] Molent, L., S.A. Barter, P. White, and B. Dixon. “Damage tolerance demonstration testing for the Australian F/A-18”. *International Journal of Fatigue*, 31:1031–1038, 2009. ISSN 0142-1123.

[27] MTS systems corporation. “MTS 810 Test Systems”. 100-154-137, 2006.

[28] Pao, P.S., P.S. Gill, and C.R. Feng. "On fatigue crack initiation from corrosion pits in 7075-T7351 aluminum alloy". *Scripta Materialia*, 43:391–396, 2000.

[29] Ro, Y., S.R. Agnew, G.H. Bray, and R.P. Gangloff. “Environment-exposure-dependent fatigue crack growth kinetics for Al–Cu–Mg/Li”. *Materials Science and Engineering A*, 468-470:88–97, 2007.

[30] Roberge, P.R. Corrosion Engineering: Principles and Practice. McGraw-Hill, 2008.

[31] Sankaran, K. K., R. Perez, K.V. Jata. “Effects of pitting corrosion on the fatigue behavior of Al alloy 7075-T6: modeling and experimental studies." Air Force Research Laboratory, WPAFB, OH, 2000.

[32] Schmutz, P. Laboratory for joining technologies and corrosion. EMPA Dubendorf, 2013.

[33] Szklarska-Smialowska, Z. “Pitting corrosion of Al”. *Corrosion Science,* 41:1743–767, 1999. ISSN 0010-938X.

[34] Uhlig, H.H. and R. Winston Revie, Corrosion and Corrosion Control, 1985.

[35] Various. Metals handbook, Vol.2 - Properties and Selection: Nonferrous alloys and special-purpose materials. ASM International, 1990.

[36] Wang, Q.Y, N. Kawagoishi, and Q. Chen. “Effect of pitting corrosion on very high cycle fatigue behavior”. *Script a Material*, 49(7):711–716, 2003.

[37] White, P., S.A. Barter, and C. Wright. “Small crack growth rates from simple sequences containing under loads in AA7050-T7451”. *International Journal of Fatigue*, 31:1865–1874, 2009. ISSN 0142-1123.

[38] Xu-Dong, L., W. Xi-Shu, R. Huai-Hui, C. Yin-Long, and M. Zhi-Tao. “Effect of prior corrosion state on the fatigue small cracking behaviour of 6151-T6 Al alloy”. *Corrosion Science*, 55:26–33, 2012.

REPORT DOCUMENTATION PAGE

Form Approved
OMB No. 074-0188

1. REPORT DATE *(DD-MM-YYYY)*	**2. REPORT TYPE**	**3. DATES COVERED** *(From – To)*
23-06-2014	Master's Thesis	August 2012 – September 2014

TITLE AND SUBTITLE

Crack initiation and growth behavior at corrosion pit in 2024-T3 aluminum alloy

5a. CONTRACT NUMBER

5b. GRANT NUMBER

5c. PROGRAM ELEMENT NUMBER

6. AUTHOR(S)

Al-Qahtani, Ibrahim, 1st Lt , Royal Saudi Air Force.

5d. PROJECT NUMBER

5e. TASK NUMBER

5f. WORK UNIT NUMBER

7. PERFORMING ORGANIZATION NAMES(S) AND ADDRESS(S)
Air Force Institute of Technology
Graduate School of Engineering and Management (AFIT/EN)
2950 Hobson Way
Wright-Patterson AFB OH 45433-7765

8. PERFORMING ORGANIZATION REPORT NUMBER

AFIT-ENY-T-14-S-05

9. SPONSORING/MONITORING AGENCY NAME(S) AND ADDRESS(ES)
Rich Hays
Technical Corrosion Collaboration
Office of Secretary of Defense
Washington D.C.
1001 30TH ST., NW Washington, D.C 20007.
2022981543.

10. SPONSOR/MONITOR'S ACRONYM(S)
TCC
OSD

11. SPONSOR/MONITOR'S REPORT NUMBER(S)

12. DISTRIBUTION/AVAILABILITY STATEMENT
DISTRUBTION STATEMENT A. Approved for Public Release; Distribution Unlimited.

13. SUPPLEMENTARY NOTES
This material is declared a work of the U.S. Government and is not subject to copyright protection in the United States.

14. ABSTRACT

In this research, fatigue crack formation from two types of corrosion pits at a circular hole was investigated under uniaxial fatigue. Through pits and corner pits were created on the edge of a circular hole in test specimens using an electrochemical process. Specimens of 2024-T3 aluminum alloy were subjected to cyclic uniaxial loads with stress ratio of R = 0.5 in both air and saltwater environments. A fracture mechanics approach was used to investigate the crack initiation and crack growth from corrosion pits. Specimens with a through pit at the edge of a circular hole had a closed form solution to predict stress intensity factor range, ΔK, which was in agreement with finite element analysis. In addition, specimens with a corner pit do not have a closed form solution and finite element modeling was used to determine stress intensity range. Optical and electron microscopy provided an accurate method to measure the size of corrosion pits. Exposure to saltwater reduced the number of cycles for crack initiation in both types of corrosion pits. This reduction is up to 90% for through pits and up to 75% for corner pits. The required number of cycles for crack initiation for corner pit specimens is less than for through pit specimens. Here, the number of cycles decreases up to 94% in air and up to 88% in saltwater environment. There was a good agreement between crack growth rates in machined notch specimens and the specimen with through pit.

15. SUBJECT TERMS
Corrosion, Fatigue, Fracture Mechanics, Crack Initiation, Crack Growth Rate, Aluminum Alloys

16. SECURITY CLASSIFICATION OF:			**17. LIMITATION OF ABSTRACT**	**18. NUMBER OF PAGES**	**19a. NAME OF RESPONSIBLE PERSON**
a. REPORT	**b. ABSTRACT**	**c. THIS PAGE**			Shankar Mall, Ph. D. (ENY)
U	**U**	**U**	**UU**	101	**19b. TELEPHONE NUMBER** *(Include area code)* (937) 255-6565, ext 4587; Shankar.Mall@afit.edu

Standard Form 298 (Rev. 8–98)
Prescribed by ANSI Std. Z39.18